Chapter 5 Effect of capping agents on gel formation and uptake of organic solvents by metallogels derived from 1,10- phenanthroline containing tricopper (II) complex

5.1 Introduction

The metallogels[1] as described in the previous chapters have been synthesized using copper(II) salts along with myo-inositol as central moiety and 2,2'-bipyridine as capping ligands. The attempts to lower the pH at which the gels are formed was also successful. The gel formation and their properties have been found to depend on the nature of the anions present as well as the metal ions. It was thought of interest to see the effect of variation in the composition of gel-forming complex cation on the formation of metallogels and their properties. As the formation of 1D supramolecular assembly is thought to be important for gel formation, core of the complex cation was kept intact and the variation was made in the peripheral moieties, i.e., the capping agents. The present chapter describes the results of attempts to vary the capping agents and the consequences of the same on different properties of the metallogels.

The supramolecular gelator systems are formed because of the non-covalent[2–8] interactions like H-bonding and π-π stacking[9–11]. Thus, any change in the organic framework of the ligands or even the type, nature and oxidation state of the metal salts used for synthesis leads to a drastic change on the metallogelator systems. Along with non-covalent interactions the role of solvent in gel formation is also significant. Usually, a particular gelator system is classified as hydrogel or organogel depending on the type of the solvent that the system can incorporate. However there have been very few reports where a gelator molecule can incorporate a variety of different solvents. In fact, such reports with metallogels are even more scarce. The ability to potentially choose a desired solvent to tune and tailor both the gel properties and suitability for different applications could be an extremely powerful approach. In one such report Fluorenyl methoxycarbonyl diphenylalanine was used as a gelator molecule to gelate various solvents ranging from water to other organic solvents. It was reported by the authors that the type and the quantity of the solvent governs the rheological properties of the gelator systems. The authors mention that the gels formed with ethanol as a solvent had the maximum mechanical strength but the poor ability to recover from shear cessation. On the hand the gels formed using DMSO had very good ability of recover but the mechanical strength of these gels was poor. The studies reported by the authors shows that using different type and quantity of solvents it is possible to fine tune the properties of the metallogels.[12]

The properties of the metallogelator systems reported in the current work are dependent on a number of factors viz. copper salts used as starting material, the nature and structure of capping ligands as well as the central moiety; the type of base used to increase the pH as well as the solvent used contributes in deciding the stability, behaviour and properties of the metallogelator systems. In this chapter the consequences on the properties of the metallogels as a result of variation in the capping the ligands have been reported.

The metallogels were synthesized using the schemes similar to what have been reported in the earlier chapters. However, as the capping ligands are changed the reaction conditions like temperature and pH as well as the volume of solvent have to be optimized. 1,10-phenanthroline and its derivatives were used as capping ligands instead 2,2'-bipyridine.

The reaction conditions like temperature and pH, volume of solvent was optimized and gels were synthesized using 1,10-phenanthroline, neocuproine (2,9-dimethyl-1,10-phenanthroline) and 3,4,7,8-tetramethyl-1,10-phenanthroline as capping ligands instead of 2,2'-bipyridine.

Caustic alkalis as well as carbonate bases were used to make the pH alkaline which is required for the coordination of myo-inositol.

As the variations in the organic framework of the gel is changed there by changing the extent of non-covalent interactions, the uptake capacity of gels was studied in presence of different solvents. The metallogels reported in this chapter have capping ligands which have more organic character as compared to 2,2'-bipy. Thus, it was thought of exploring the incorporation of solvents which are more non-polar as compared to water, by the metallogels. The studies and the results have been discussed further in the chapter.

5.2 Experimental section

5.2.1 Materials

Cupric acetate monohydrate, 1,10-phenanthroline and neocuproine (2,9-dimethyl-1,10-phenanthroline) were purchased from Qualigens. 5-Nitro-1,10-phenanthroline, 3,4,7,8-tetramethyl-1,10-phenanthroline, biquinoline and myo-inositol (ins) were procured from Sigma-Aldrich. 6,6'-Dimethyl-2,2'-bipyridine was procured from TCI. K_2CO_3, Na_2CO_3 and KOH were purchased from Qualigens. Cupric formate was prepared using formic acid and cupric carbonate. NaOH and formic acid were obtained from Merck.

Reagent grade cupric carbonate was procured from local manufacturer. All the chemicals were of AR or GR grade and were used for synthesis without further purification. Cupric formate was prepared by reacting formic acid with cupric carbonate. Triple distilled water was used as solvent for the synthesis of gels.

5.2.2 Synthesis

Synthesis of gels with hydroxide base and 1,10-phenanthroline as capping agent

The reaction of 10 mL of a 2.5% aqueous solution (1.388 mmol) of myo-inositol was carried out with 3 equivalents of $[Cu(phen)]^{2+}$ complex obtained by reacting **0.831 g (4.163 mmol)** of cupric acetate and **0.825 g (4.163 mmol)** of phen in 20 mL of water **(Scheme 5.2.2.1)**. Repeating the same procedure with cupric formate **(0.638 g, 4.163 mmol)** resulted in the formation of green transparent gel-**221**. Subsequently, the pH was raised to 12 with aqueous potassium hydroxide. The solution was held at 60–70 °C for 30 minutes and allowed to settle at room temperature to obtain the gel **(222)**.

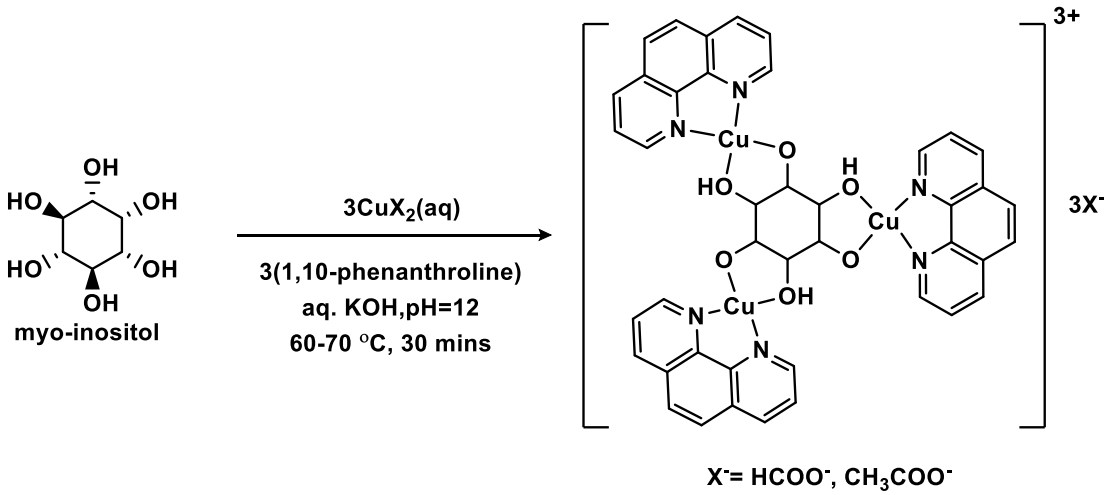

Scheme 5.2.2.1 Synthesis of the trinuclear copper (II) complex hydrogelator synthesized using myo-inositol and 1,10-phenanthroline in presence of KOH.

Synthesis of gel with carbonate base and 1,10-phenanthroline as capping agent

The reaction of 10 ml 2.5% aqueous solution **(1.388 mmol)** of myo-inositol was carried out with 3 equivalents of $[Cu(phen)]^{2+}$ complex obtained by reacting **0.638 g (4.163 mmol)** of cupric formate and **0.825 g (4.163 mmol)** of phen in 20 ml water **(Scheme 5.2.2.2)**. Subsequently, the pH was raised to **8.5** by adding a solution of aqueous K_2CO_3 to the above reaction medium. The solution was heated in oven at 95 °C for 90 minutes after which gel formation takes place **(232)**. Repeating the same procedure with cupric acetate **(0.831 g, 4.163 mmol)** instead of cupric formate as the starting material, resulted

in the formation of green transparent gel-**231**. The same procedure was repeated using equivalent amounts of all reagents but using aqueous sodium carbonate as base in place of potassium carbonate to get the gels **251** and **252** with cupric formate and copper acetate, respectively.

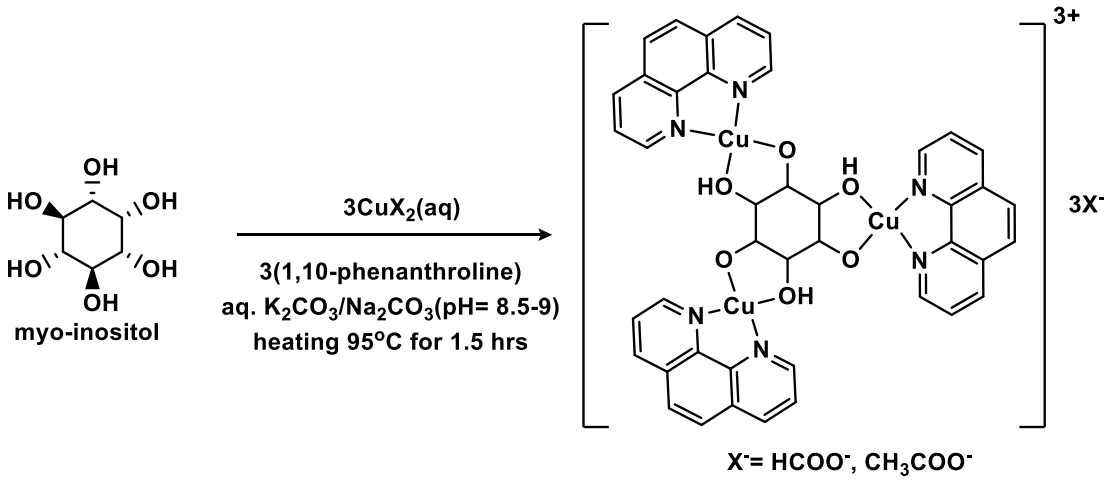

Scheme 5.2.2.2. Synthesis of the trinuclear copper (II) complex hydrogelator synthesized using myo-inositol and 1,10-phenanthroline in presence of carbonate base.

Synthesis of gels with carbonate base and neocuproine as capping agent

The reaction of 1 equivalent of myo-inositol with 3 equivalents of copper acetate and 3 equivalents of **neocuproine (2,9-dimethyl-1,10-phenanthroline) (neo)** was carried out in order to yield the metallogel **332**. The reaction of 10 ml 2.5% aqueous solution **(1.388 mmol)** of myo-inositol was carried out with 3 equivalents of **[Cu(neo)]**$^{2+}$ complex obtained by reacting **0.831 g (4.163 mmol)** of cupric acetate and **0.867 g (4.163 mmol)** of **neo** in 20 ml water **(Scheme 5.2.2.3)**. Subsequently the pH was raised to **8.1** by adding a solution of aqueous K_2CO_3 to the above reaction medium. The solution was heated in oven at 95 °C for 75 minutes post which gel formation takes place (**332**). The gelation was confirmed by the inverted test tube method.

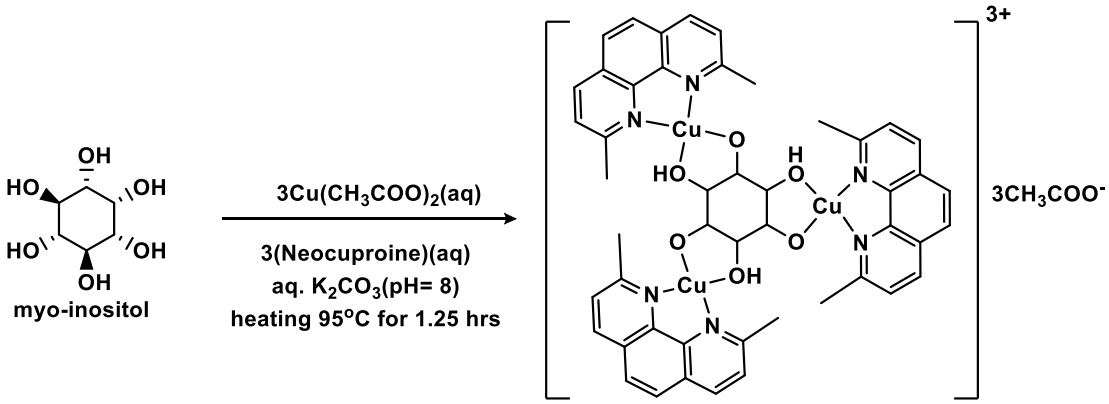

Scheme 5.2.2.3 Synthesis of the trinuclear copper (II) complex hydrogelator synthesized using myo-inositol and Neocuproine.

Table 5.2.2.1 Codes and Composition of the metallogels

Code	Capping Ligand	Counter Anion	Base
221	phen	Formate	KOH
222	phen	Acetate	KOH
231	phen	Formate	K_2CO_3
232	phen	Acetate	K_2CO_3
251	phen	Formate	Na_2CO_3
252	phen	Acetate	Na_2CO_3
332	Neocuproine	Acetate	K_2CO_3

Synthesis of gels using various other capping agents

Cupric acetate monohydrate and potassium carbonate were selected as starting compounds and base, respectively, for examining the gel formation in presence of other capping agents. The same procedure as for the synthesis of **232** and **332** was followed using equivalent amounts of 5-Nitro-1,10-phenanthroline, 3,4,7,8-tetramethyl-1,10-phenanthroline, biquinoline and 6,6'-Dimethyl-2,2'-bipyridine were used in place of 1,10-phenanthroline or neocuproine. Either K_2CO_3 (pH = 8.5-9) or KOH (pH = 12) were used to maintain the pH. The observations are listed in **Table 5.3.1.1.**

5.2.3 Instrumentation and Techniques

UV-Visible: UV–vis spectroscopy was used to monitor the gel formation as well as for recording the spectra of metallogels. Perkin Elmer Lambda 35 dual beam UV–vis Spectrophotometer was used for the purpose.

T_{gel}: Sol-gel transition temperatures, T_{gel}, of the gels were measured using a Julabo 5 A thermostat with a temperature controller and a thermometer with an accuracy of ±0.05 °C. Gels were taken in screw capped glass vials and immersed in a water bath whose temperature was gradually increased by a temperature control program and the T_{gel} temperatures of the gels were recorded using the inverted test-tube method.

FTIR: FTIR spectra of xerogels were recorded using a Bruker Alpha FT-IR) spectrometer in solid state as KBr pellets.

Mass spectrometry: The ESI mass spectra of the hydrogels were recorded using Applied Biosystem API 200 mass spectrometer.

ESR: ESR of the metallogelator complexes were recorded using E-112 VARIAN USA spectrometer in solution phase (H_2O) at RT using X- band frequency (9.45 GHz).

Computational Studies: Full geometry optimizations were carried out using density functional theory (DFT) with B3LYP[13–16] and LANL2DZ[17,18] basis set. Gaussian 16[19] and Gauss View 6[20] programs for computation and visualization of output.

Scanning electron microscopy (SEM): SEM analysis was performed using a JEOL JSM-5610 instrument. Xerogels were prepared on SEM stubs for capturing the SEM images.

Polarizing optical microscopy (POM): Microscopic analysis under polarized light analysis was performed using a LEICADM2500P polarizing microscope. Images were captured using a LEICADFC295 camera, which is attached to the instrument. Images were processed using the software LAS V4.1. A thin layer of gel was formed on a glass slide and allowed to dry and get converted to a xerogel whose images were captured at various magnifications and different angles of the polarizer

5.3 Results and Discussion

5.3.1 Effect of variation in capping agents on gelation

As mentioned earlier, it was thought of interest to make variation in the gel forming tricopper(II) complex ion itself and verify its effect on the gel formation and gel properties. As myo-inositol is responsible for providing the basis for trinuclear complex formation and copper(II) forming a more stable gel among the metal ions examined, it was decided to keep the inner core intact and vary the capping agents L in the complex cation, $[Cu_3(ins)L_3]^{3+}$. As 2,2'-bipyridine could successfully yield the metallogels described in the earlier chapters, various bidentate aromatic N-bases were selected as capping agents. Variation has been made by (i) adding functional groups over the aromatic rings and (ii) increasing the size of the aromatic part of the ligands. The derivative of 2,2'-bipyridine, namely, 6,6'-Dimethyl-2,2'-bipyridine, 1,10-phenanthroline and its derivatives, namely, 5-Nitro-1,10-phenanthroline, 2,9-dimethyl-1,10-phenanthroline (neocuproine), 3,4,7,8-tetramethyl-1,10-phenanthroline and biquinoline were used. The results of gel formation experiments have been summarized in the **Table 5.3.1.1.** In all the gelation trails mentioned in the table below copper(II) acetate was using as starting material. Potassium carbonate or KOH were used as base in order to make the pH alkaline.

Table 5.3.1.1 Results of gelation trails by variation in capping agents

Capping Ligand	Result with KOH	Result with K_2CO_3
1,10-phenanthroline	**Gel**	**Gel**
Neocuproine	**Gel**	**Gel**
3,4,7,8-tetramethyl-1,10-phenanthroline	**Gel**	**Gel**
5-Nitro-1,10-Phenanthroline	No gel	No gel
Biquinoline	No gel	No gel
6,6'-Dimethyl-2,2'-bipyridine	**Gel**	**Gel**

Changing 2,2'-bipyridine to 1,10-phenanthroline helped the gel formation, however, further increase in the bulk and aromaticity by changing it to biquinoline was not helpful. It resulted in precipitation rather than gel formation. It appears that addition of simple methyl groups on the amine ligand does not

affect the gel formation. Probably because it just adds to the hydrophobicity of the exterior part of the complex and therefore is still helpful in the formation of gels. Further the presence of nitro- group in 5-nitro-1,10-phenanthroline adversely affects the gel formation. It may be because of (i) increase in polarity of the exterior, (ii) providing additional H-binding sites at the periphery and (iii) decrease in the symmetry.

The metallogelator complexes, **$[Cu_3(H_3ins)(phen)_3]X_3$** was also synthesized using both, caustic alkali like KOH and carbonate base as well as the X has been varied as $HCOO^-$(**221**) and CH_3COO^-**(222)**. The gels synthesized using KOH were not much explored further for applications as the pH at which they were formed is fairly high (pH=12). On the other hand, the metallogels using carbonate bases are formed at a much lower pH which makes them desirable candidates for biological and other applications. Hence, these were studied further in detail.

The supramolecular metallogels have been prepared using metallogelator complexes, **$[Cu_3(H_3ins)(phen)_3]X_3$**, X = $HCOO^-$**(231, 251)**, CH_3COO^-**(232, 252)** and K_2CO_3 **(231, 251)** or Na_2CO_3 **(251, 252)** as alkali at pH **8.5 (Scheme 5.3.2.2).** Apart from 1,10-phenanthroline, **2,9-dimethyl-1,10-phenanthroline (Neocuproine)** was also used as a capping ligand and the gel formation was achieved in presence of potassium carbonate as base.

5.3.2 UV-Visible spectroscopy

The UV-Visible spectra of the metallogelator complexes **222, 231, 232** and **332** were recorded before and after the formation of the gels. **(Figure 5.3.2.1 and Figure 5.3.2.2)**. The complex ion responsible for the formation of metallogels in presence of KOH **(222)** and carbonate bases i.e., Na_2CO_3 **(252)** and K_2CO_3 **(232)** is the same having the formula **$[Cu_3(H_3ins)(phen)_3]^{3+}$**. Hence, those with K_2CO_3 were considered as representatives.

First the UV-Visible spectrum of the ternary complex solution (copper acetate + phen + myo-insoitol taken in appropriate ratio) in presence of potassium carbonate before gel formation was recorded. This was followed by recording the UV-Visible spectrum of the metallogel formed as a result of heating the ternary complex as mentioned in the **Scheme 5.2.2.2.** This also leads to a change in the coordination sphere of the metal ions which is confirmed by the shift observed in the ligand field band in their UV-Visible spectra**.** It is observed that

there is a shift in the λ_{max} from a blue-coloured gel forming copper complex having absorption maximum at **642 nm** to a green-coloured gel having an absorption maximum at **672 nm (Figure 5.3.2.1)**. In the metallogel-**232** reported here, the copper(II) center is coordinated to 1,10-phenanthroline and myo-inositol. The coordination of myo-inositol takes place in alkaline medium, either in presence of carbonate bases **(232** and **252)** or hydroxide base **(222)**, post heating. The shift in the λ_{max} is a result of the change in the coordination sphere of the metal center due to the formation of a supramolecular assembly. In a similar manner the d-d transition and molar absorptivity values were determined for other metallogels **(Table 5.3.2.1)**.

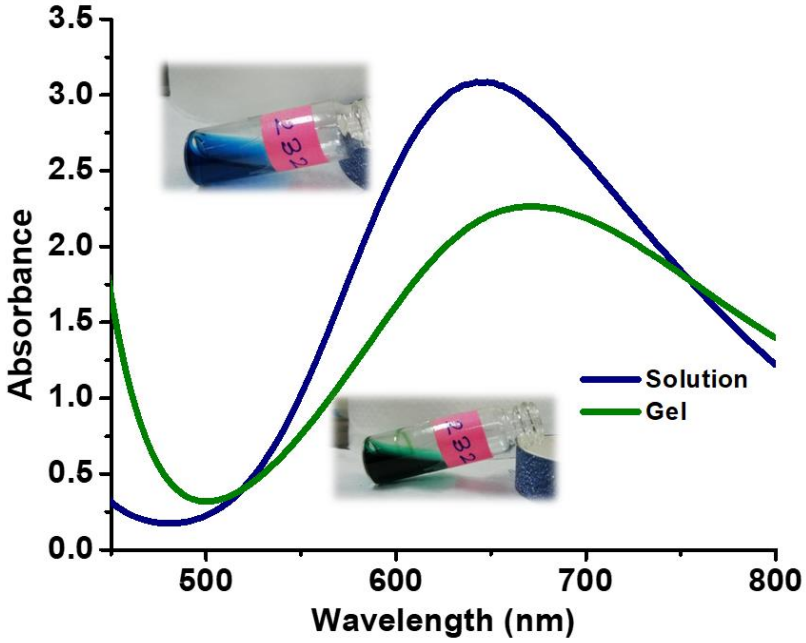

Figure 5.3.2.1 The UV-visible spectra of the metallogel **232 (in solution state)** and its solution before gel formation (before heating).

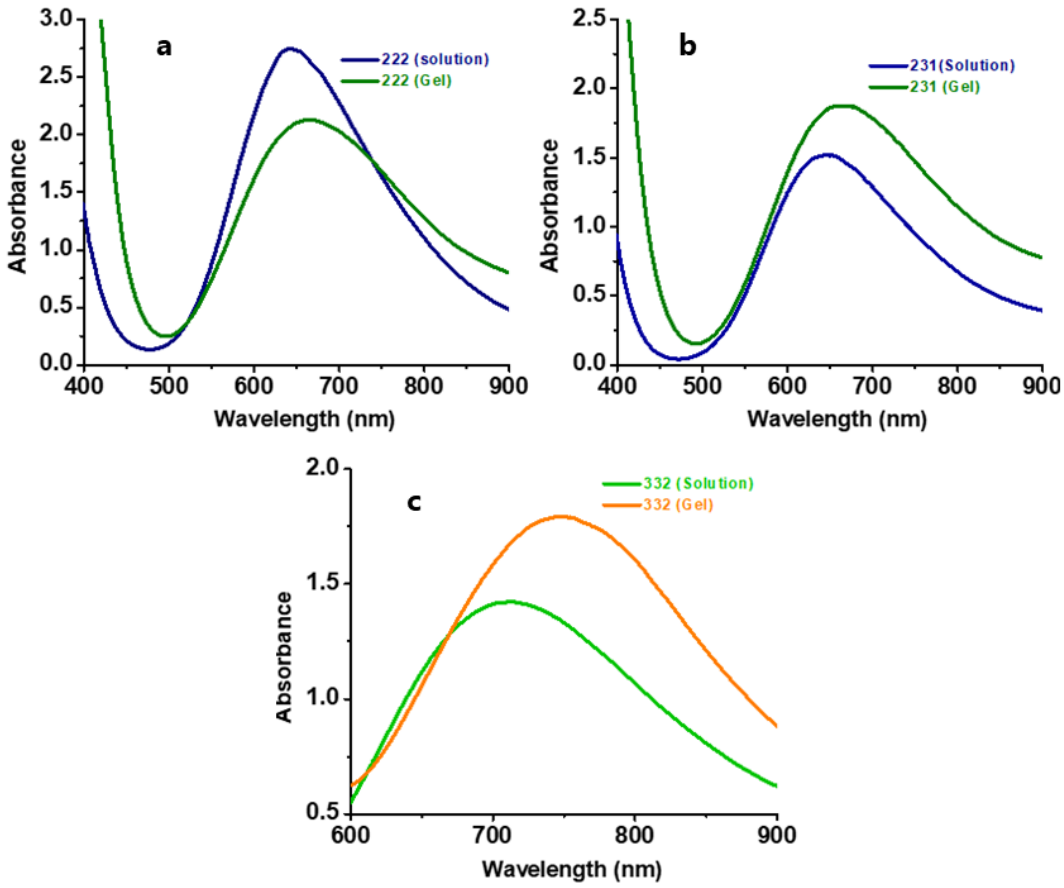

Figure 5.3.2.2 The UV-visible spectra of the metallogel **(a) 222 (b) 231** and **(c) 332** and the corresponding solutions before gel formation.

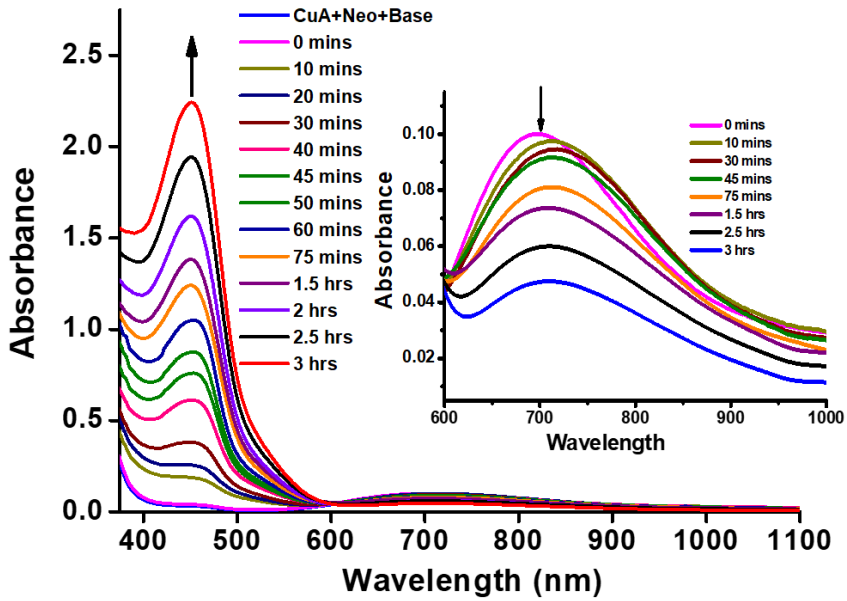

Figure 5.3.2.3 The UV-visible spectra of the metallogel complex-**332** and its solution before gel formation.

Table 5.3.2.1 λ_{max} and ε values of the metallogels

Codes of gel/solution	λ_{max} (nm) (d-d transitions)	ε -Molar absorptivity extension coefficient ($M^{-1}cm^{-1}$)
222-solution	**645**	**215**
222-gel	**670**	**220.91**
231-solution	**645**	**161**
231-gel	**665**	**142**
232-solution	**645**	**219.66**
232-gel	**672**	**225**
332-solution	**710**	**212.74**
332-gel	**745**	**268.37**

5.3.3 Sol-Gel Transition temperature (T_{gel})

Gels are a heterogeneous system formed by an immobile network of the solid incorporating a mobile solvent. Consequently, the gels possess a solid like property that can sustain shear and stress which varies from system to system. At the gelation point an infinite cluster is created that spans the whole system and the system assembles into a gel having solid like property. The gelator systems are sensitive to temperature changes. When the gels are subjected to an elevated temperature the macroscopic properties change abruptly from solid like to liquid like property. The temperature at which this transformation of the gel to a solution like behavior is called Sol-Gel temperature, also referred to as T_{gel}.[1]

The formation of the gels is characterized by inverted vial experiment and T_{gel} temperature. The metallogels formed using phenanthroline and its derivatives as capping agent were susceptible to thermal changes and T_{gel} temperatures were recorded for all the gels reported here, in this chapter. The variation in the capping ligands, the counter ion, alkyl carboxylates and the alkali used for maintaining the pH leads to a significant change in the solvent uptake capacity and the T_{gel} values of the metallogels **(Table 5.3.3.1)**.

The gels prepared using Na_2CO_3 as a base have slightly higher T_{gel} values **(232 and 252)** than the gels prepared using K_2CO_3 **(231 and 251)**. This trend is similar to the

metallogels synthesized using 2,2'-bipyridine as capping ligand in presence of carbonate bases. However, the T_{gel} values of the metallogels prepared using 1,10-phenanthroline as a capping ligand are significantly lower than those containing 2,2'-bipyridine **(Table 5.3.3.1)**. The carboxylate anions also have a significant effect on the gel properties. The gels synthesized using formate have consistently lower T_{gel} values as compared to those containing acetate. However, this trend is reversed when the gels are synthesized using KOH as a base, the gels having acetate **(222)** as counter anion have higher T_{gel} as compared to the ones containing formate **(221)**.

While the change from 2,2'-bipyridine to 1,10-phenanthroline resulted in significant lowering in the T_{gel} values, the change from 1,10-phenanthroline to neocuproine does not have significant effect on the T_{gel} values.

It was observed that as the capping ligands are changed from 2,2'-bipyridine to 1,10-phenanthroline or neocuproine the water retention capacity as well as the T_{gel} values of the metallogels are significantly lowered. This can be seen in the values in column 3 and 4 of the **Table 5.3.3.1.**

Table 5.3.3.1 Optimum water retention capacity and the T_{gel} values of the metallohydrogels.

Gel codes	Optimum-water retention capacity per 100 mg of xerogel	T_{gel} (°C) phen and neocuproine as capping ligand	T_{gel} (°C), with capping ligand as bipy*
221	0.653 mL	**37 ± 0.5**	**39.5** ± 0.5 **(121)**
222	0.655 mL	**39 ± 0.5**	**43.5** ± 0.5 **(122)**
231	0.653 mL	**42 ± 0.5**	**77** ± 0.5 **(131)**
251	0.653 mL	**44 ± 0.5**	**88** ± 0.5 **(151)**
232	0.655 mL	**37 ± 0.5**	**47** ± 0.5 **(132)**
252	0.655 mL	**39 ± 0.5**	**55** ± 0.5 **(152)**
332	0.641mL	**37.5 ± 0.5**	**47** ± 0.5 **(132)**

**The last column mentions the T_{gel} values for the metallogels reported in Chapter 2 and 4.*

The numbers in the parenthesis in the last column correspond to the codes of the gels.

5.3.4 FTIR Spectroscopy of Xerogels

The metallogels were dried and converted to xerogels in order to record their FTIR spectra. The FTIR spectra (KBr) of xerogels exhibited important strechings of both myo-inositol and phen. Among these, the aliphatic C-H stretching vibrations at 2700-3000 cm^{-1}, the C-C multiple bond stretching and the ring C-N vibration in phen between 1400-1600 cm^{-1} were prominent. The presence of absorptions at ~1136-1145, 1031, 995-1005 and 840-855 cm^{-1} supported the coordination of phen while the absorptions at ~1100, 730 and 660 cm^{-1} supported the presence of coordinated inositol **(Figure 5.3.4.1 to Figure 5.3.4.6)**. Thus, the residue obtained after washing was expected to be the corresponding ternary complex As the ternary complex **$[Cu_3(H_3ins)(phen)_3]X_3$,** where **$X=HCOO^-$(231, 251), CH_3COO^-(232, 252)**, present in the xerogel remained the same, the FT-IR spectrum of the xerogels resemble with each other, except for the presence of counter anions and showed the prominent vibrations as discussed above. As the counter anions were varied during the study, the vibrations corresponding to the counter anions, namely, formate and acetate were different amongst the xerogels discussed.

The metallogel **332** formed using the similar scheme having neocuproine as the capping agent was converted into xerogel. However, the xerogel could not be completely dried and its FT-IR spectrum could not be recorded.

FT-IR data for xerogels:

Xerogel-231: FT-IR, cm^{-1} (KBr): 3417.42, 2817.59, 2727.39, 1590.78, 1518.00, 1426.59, 1381.92, 1348.99, 1223.52, 1145.11, 1105.88, 1050.70, 1031.98, 1005.14, 954.65, 893.73, 849.74, 778.78, 722.96, 647.18, 590.08, 429.55.

Xerogel-251: FT-IR, cm^{-1} (KBr): 3432.22, 3047.35, 2924.84, 2814.29, 2780.25, 1625.75, 1505.69, 1421.07, 1348.68, 1220.49, 1136.19, 1048.55, 1000.99, 838.68, 770.66, 720.47, 588.64, 426.80.

Xerogel-232: 3444.09, 3363.22, 3057.66, 2885.03, 2828.41, 1651.59, 1607.27, 1519.31, 1492.17, 1430.21, 1403.99, 1344.95, 1308.90, 1252.88, 1220.38,1137.88, 1105.97, 1053.36, 1037.04, 995.31, 917.21, 855.72, 780.21, 737.49, 723.65, 688.74, 645.75, 626.12, 562.04, 545.70, 525.64, 485.38, 443.47, 429.20.

Xerogel-252: FT-IR, cm^{-1} (KBr): 3416.50, 3005.11, 2932.35, 2858.72, 1577.66, 1517.56, 1421.13, 1339.65, 1222.84, 1141.61, 1104.39, 1025.08, 952.92, 924.55, 847.84, 776.65, 723.16, 649.25, 621.00, 586.36, 426.96.

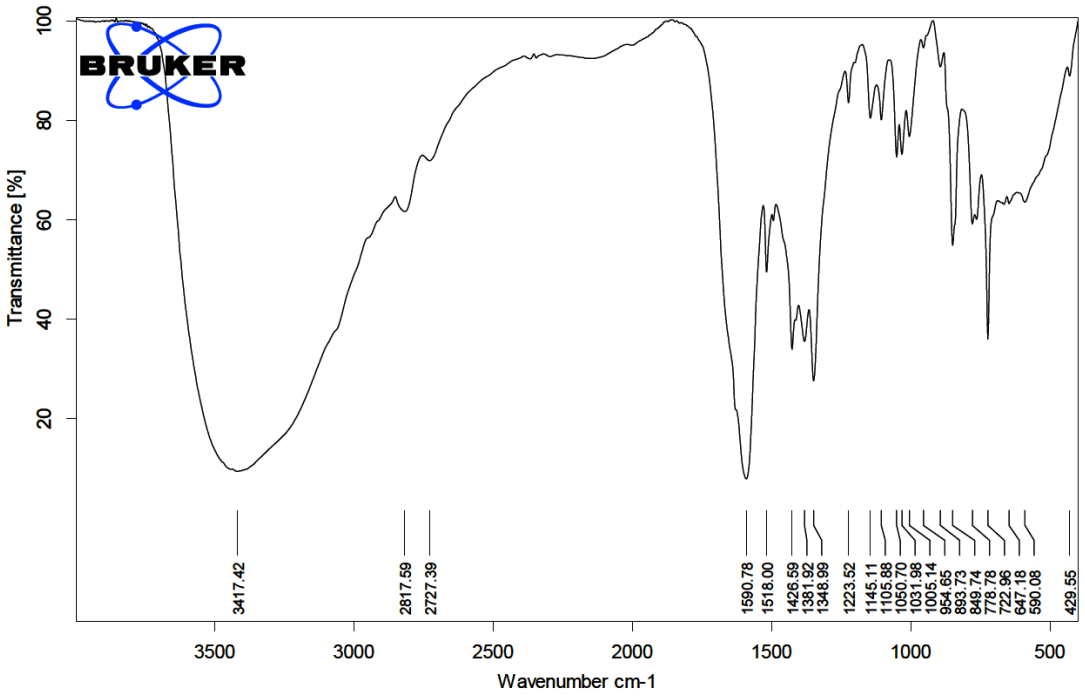

Figure 5.3.4.1 FTIR spectrum of xerogel **231.**

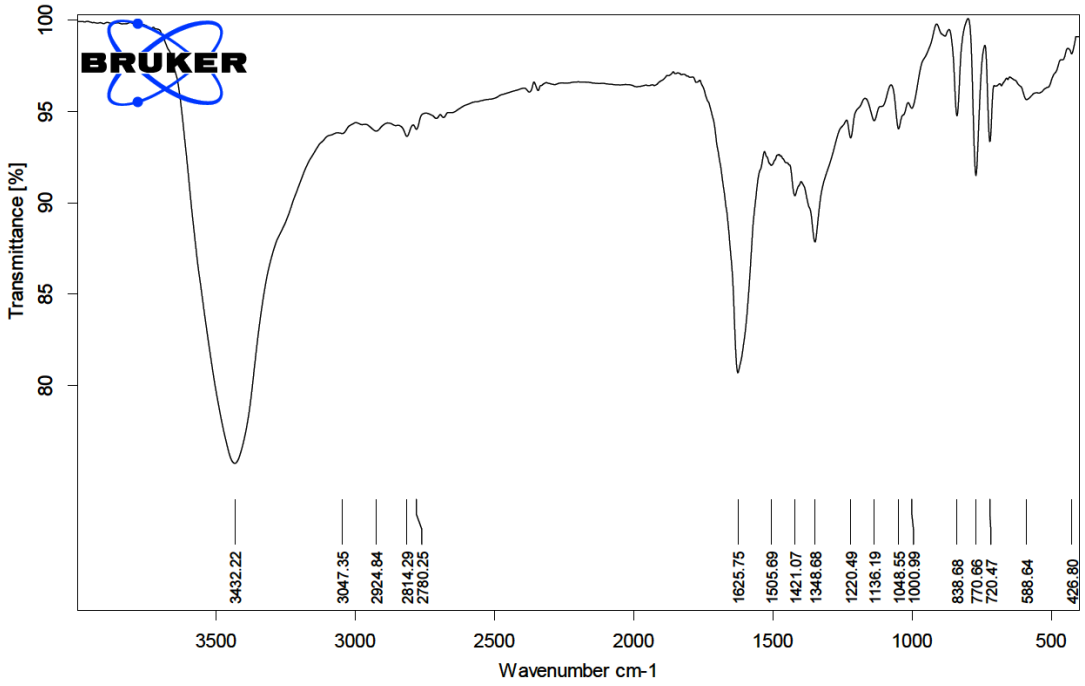

Figure 5.3.4.2 FTIR spectrum of xerogel **251.**

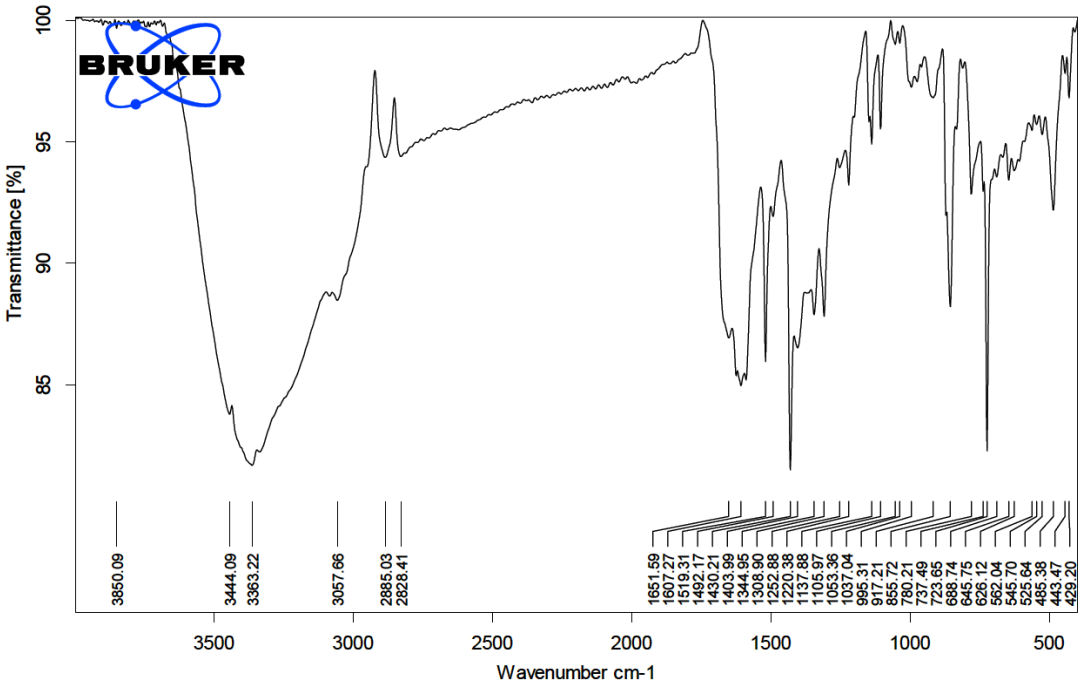

Figure 5.3.4.3 FTIR spectrum of xerogel **232.**

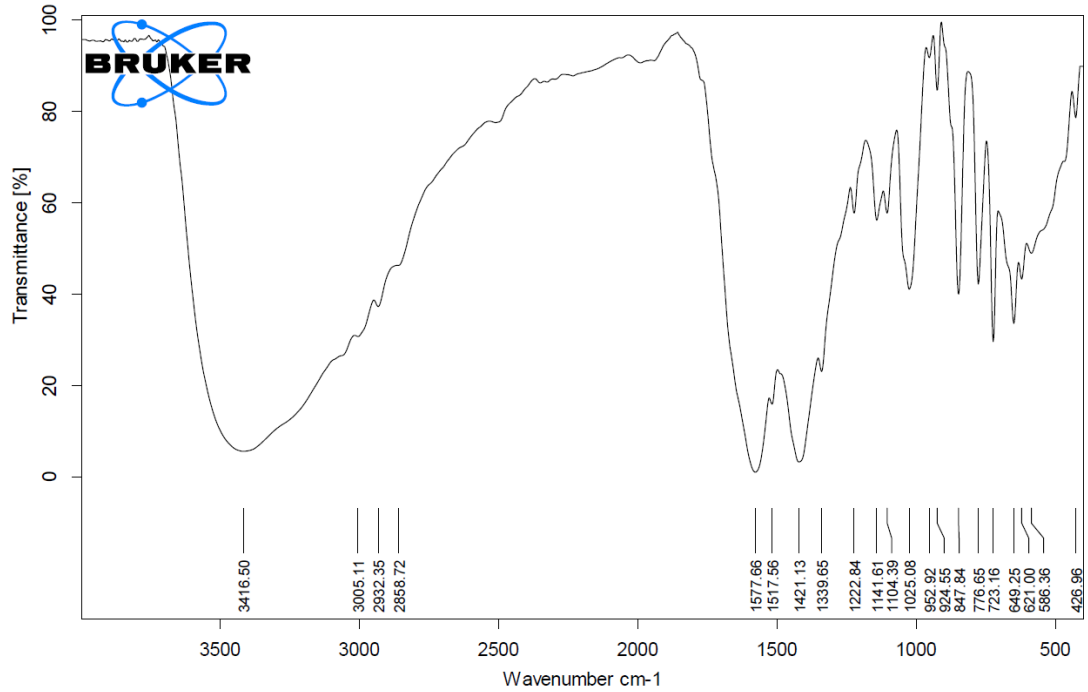

Figure 5.3.4.4 FTIR spectrum of xerogel **252.**

5.3.5 ESI-MS Analysis of Metallogels

ESI-MS Analysis of the metallogels having phen as capping agent

In order to prove the existence of the trinuclear copper(II) complex ESI-MS of the gels was carried out. The gels were formed using copper salts with 1,10-phenanthroline (phen) or neocuproine as capping ligands and myo-inositol as the central moiety. The supramolecular assemblies which result in the formation of the metallogels are formed because of the complex cation $[Cu_3(H_3ins)(phen)_3]^{3+}$ in the case of phen as capping ligand and $[Cu_3(H_3ins)(neo)_3]^{3+}$.

The gels were synthesized as mentioned in the **Scheme 5.2.2.1** and **Scheme 5.2.2.2**. The proposed metallogelator complex in both the cases is the same i.e. **$[Cu_3(H_3ins)(phen)_3]^{3+}$**, the only difference being the selection of base. Potassium hydroxide was used as a base in the synthesis of the metallogels **221** and **222**. The important peaks in the ESI-MS of both the metallogels **221 (Figure 5.3.5.1)** and **222 (Figure 5.3.5.2)** were also similar as the counter anions, formate in the case of gels **221** and acetate in the case of the gels **222,** were present outside the coordination sphere of the metallogelator complex, thus having no effect on the values of m/z ratio of the complexes. The ESI-MS of the gels **221 and 222** recorded in aqueous media has a peak with significant intensity at **m/z = 302, 304** which corresponds to the metallogelator complex cation, **$[Cu_3(H_3ins)(phen)_3]^{3+}$**. The peaks obtained at M and M+2 are related to the isotopic abundance of copper with mass numbers 63 and 65 in 3:1 ratio. The peaks at **m/z=302, 304** were observed in the mass spectra of both these gels. This supported the existence of trinuclear trication, **$[Cu_3(H_3ins)(phen)_3]^{3+}$**, which must be further undergoing H-bond formation or coordination with water molecules. In the basic medium the hydroxide must be participating in the hydrogen bonded assembly along with the anions formate or acetate present as counter anions as in the case of the metallogels reported in the earlier chapters.

The metallogels **231** and **232** were prepared using copper formate and copper acetate, respectively, in presence of potassium carbonate. Similarly, metallogels **251** and **252** were synthesized using copper formate and copper acetate respectively, in presence of sodium carbonate as a base. However, in each of these metallogels the trinuclear gel forming complex cation remains the same. Thus, the ESI-MS spectra of all 4 metallogels **(Figure 5.3.5.3** to **Figure 5.3.5.6)** indeed have peaks at m/**z=302, 304**

corresponding to the trinuclear complex cation, **$[Cu_3(H_3ins)(phen)_3]^{3+}$**, which is responsible for the gel formation.

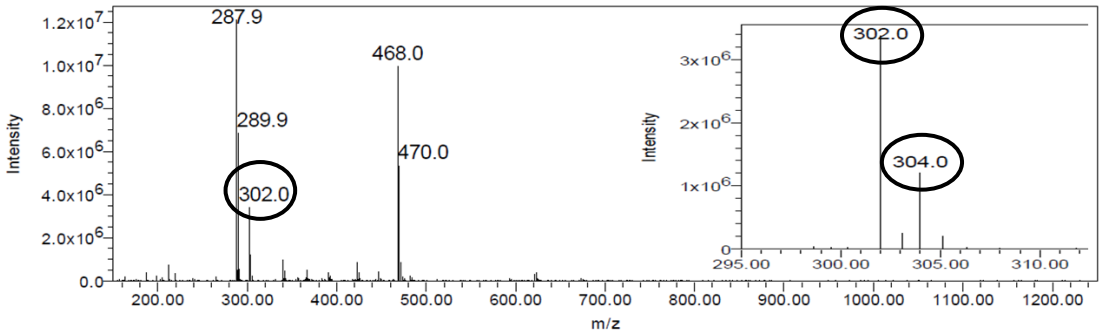

Figure 5.3.5.1 ESI-MS of the metallogel-**221**.

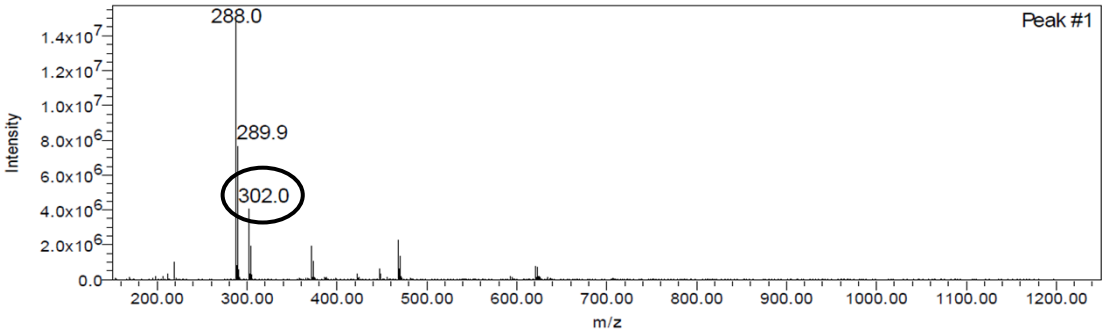

Figure 5.3.5.2 ESI-MS of the metallogel-**222**.

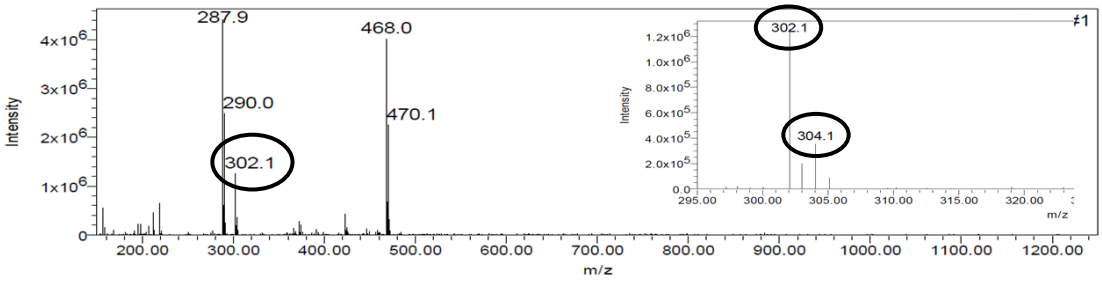

Figure 5.3.5.3 ESI-MS of the metallogel-**231**.

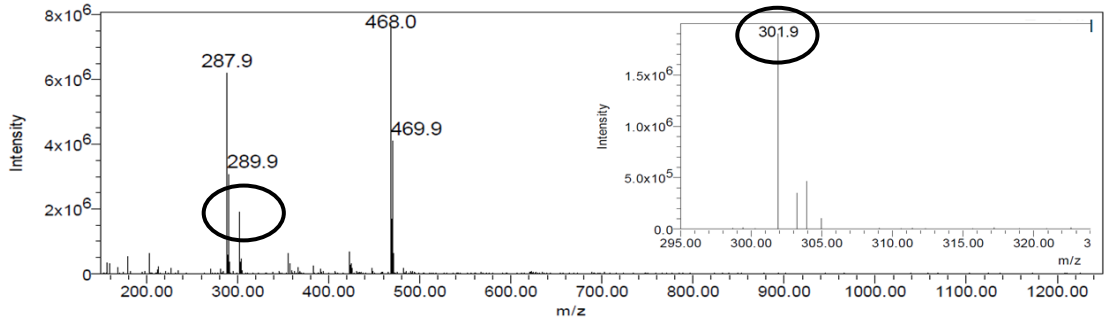

Figure 5.3.5.4 ESI-MS of the metallogel-**251**.

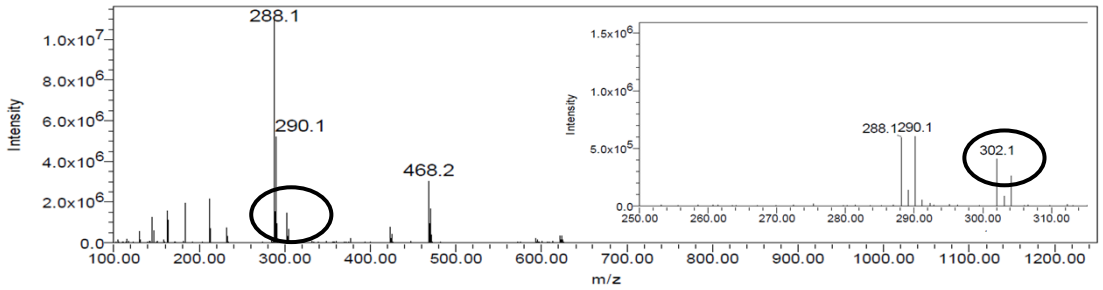

Figure 5.3.5.5 ESI-MS of the metallogel-**232**.

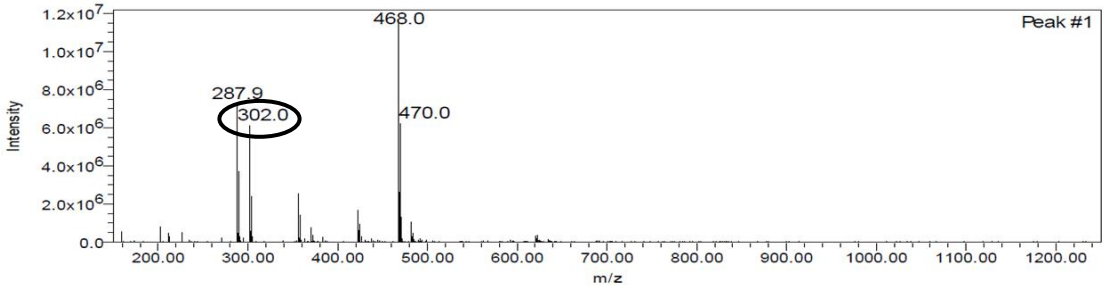

Figure 5.3.5.6 ESI-MS of the metallogel-**252**.

ESI-MS Analysis of the metallogel having neocuproine as a capping agent

The metallogel **332** was synthesized as per the **Scheme 5.2.2.3** using myo-inositol as a central moiety and neocuproine as a capping agent. The ESI-MS of the metallogel **332 (Figure 5.3.5.7)** has distinct peaks at **m/z = 329.7, 331.7** corresponding to the trinuclear complex **$[Cu_3(H_3ins)(neo)_3]^{3+}$**. Isotopic abundance of copper as in the case of other metallogelator complexes is responsible for the peaks at M and M+2.

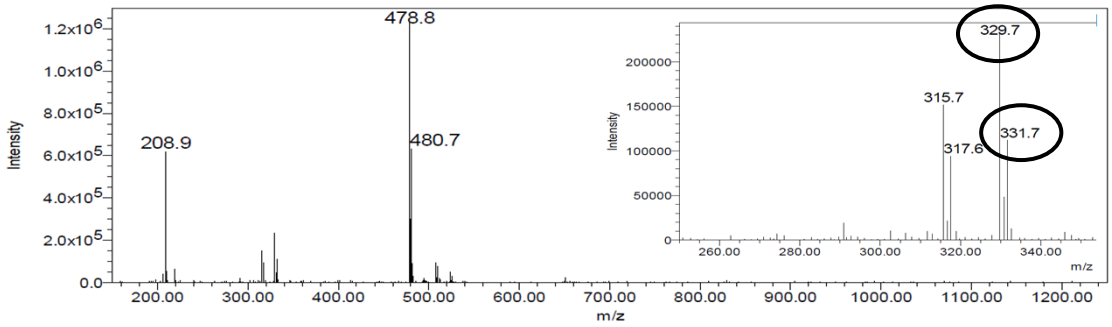

Figure 5.3.5.6 ESI-MS of the metallogel-**332**.

5.3.6 Electron Spin Resonance

The ESR spectra of metallogels were recorded in aqueous state at room temperature. These are typical spectra of copper(II), a S=1/2 system in axial ligand field. A well resolved hyperfine structure in the g|| region is observed, with four discernible lines for metallogels **231** and **232.** Metallogel **231** has $g_{\|}$ = 2.1469 and $g_{\perp}$ = 2.0729 with an average $A_{\|}$ value = 60.14 x 10^{-4} cm^{-1}. Metallogel **232** has $g_{\|}$ = 2.1469 and $g_{\perp}$ = 2.0522 and an average $A_{\|}$ value = 70.16 x 10^{-4} cm^{-1}. The metallogel **332** does not show any hyperfine splitting and has $g_{\|}$ = 2.2015 and $g_{\perp}$ = 2.1418 as seen in the **Figure 5.3.6.1.**

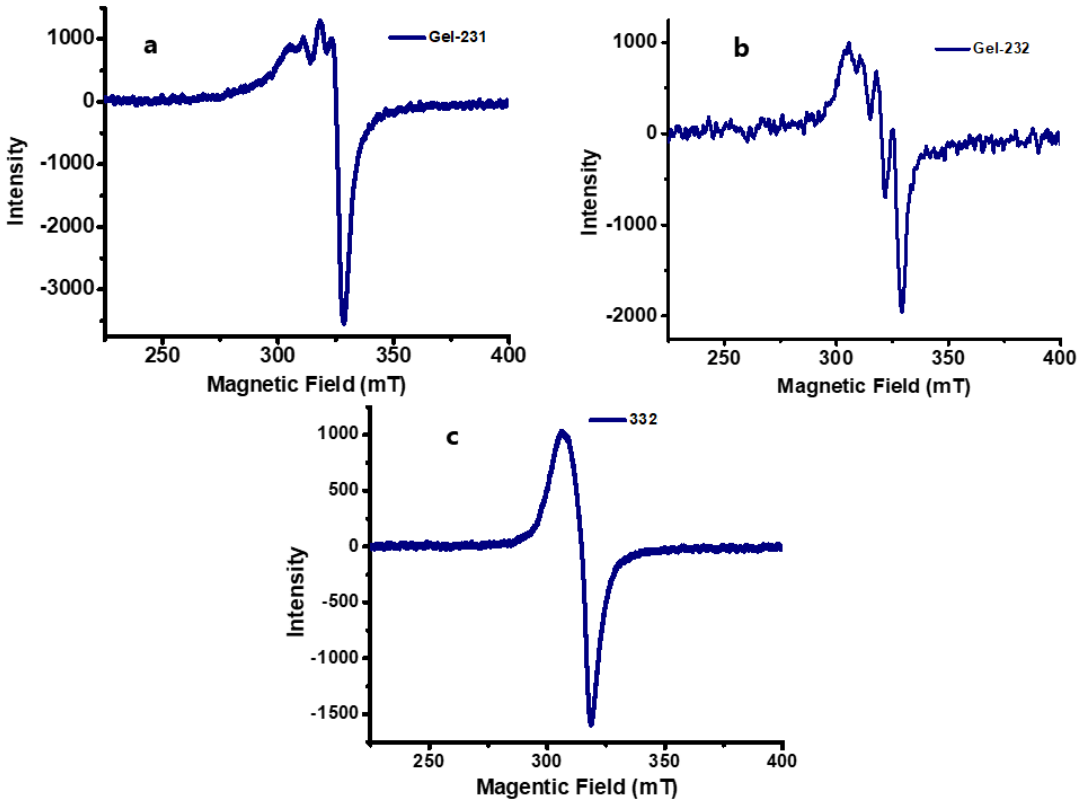

Figure 5.3.6.1 ESR spectra of the metallogels **231 (a), 232 (b)** and **332 (c)**, recorded in aqueous media at room temperature.

In the typical spectrophotometric analysis of copper using neocuproine, there are arguments of the orange-coloured species being a copper(I) complex of neocuproine[21]. However, in the ESR spectrum of the metallogel formed in presence of neocuproine, **332**, which also happened to be orange coloured, there is clear evidence of the existence of copper(II), which rules out any possibility of reduction of the cupric ion to cuprous state.

5.3.7 Computational studies of the metallogelator complexes

The complex cation **$[Cu_3(H_3ins)(phen)_3]^{3+}$** is responsible for the metallogel formation. However, in spite of numerous attempts the complex salt / molecule did not crystallize. As a result, the single crystal analysis of the complex could not be performed. FT-IR, ESI-MS supported the coordination of myo-inositol, however, to further support the bonding of myo-inositol and phen to the copper centers, it was necessary to get support from molecular modelling.

To get an insight into the structure and bonding of the gels computational studies of the complex cation-**$[Cu_3(H_3ins)(phen)_3]^{3+}$** were carried out. Attempt was made to theoretically model the trinuclear copper (II) complex cation, **$[Cu_3(H_3ins)(phen)_3]^{3+}$**. The geometry of the complex was optimized by **DFT** calculations using Gaussian 16[19] wherein B3LYP[13–16] and LanL2DZ[17,18] basis sets were used for the computation. **Figure 5.3.7.1** shows that the calculated bond distances are indeed within the range of coordinate bond lengths.

The Lowest Unoccupied Molecular Orbital (LUMO) and Highest Occupied Molecular Orbital (HOMO) act as electron acceptor and electron donor.[22] Theoretical transition energy between HOMO and LUMO frontier molecular orbitals (**Figure 5.3.7.2**) was calculated by B3LYP and LANL2DZ methods for the metallogelator complex **$[Cu_3(H_3ins)(phen)_3]^{3+}$**and is tabulated in **Table 5.3.7.1.**

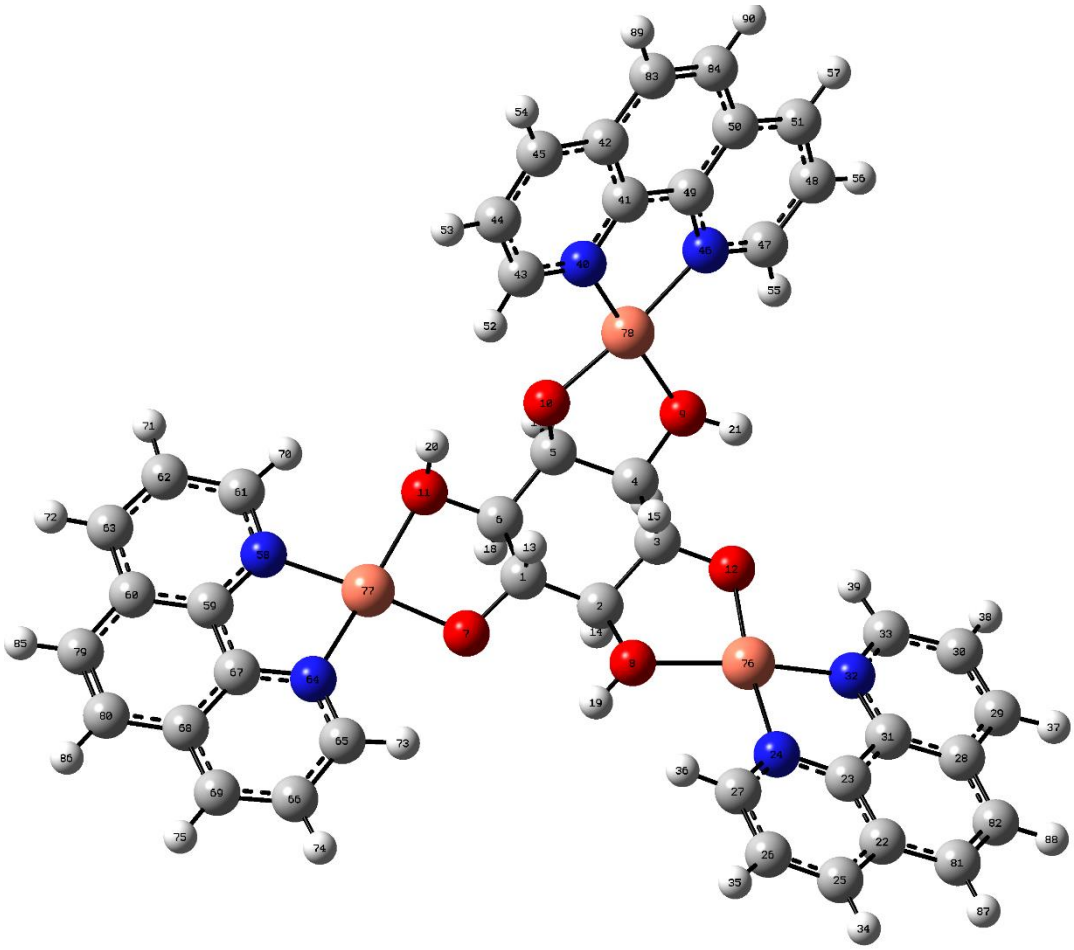

Figure 5.3.7.1 The optimized structure of the complex [$Cu_3(H_3ins)(phen)_3$]$^{3+}$using B3LYP theory and LanL2DZ as basis sets.

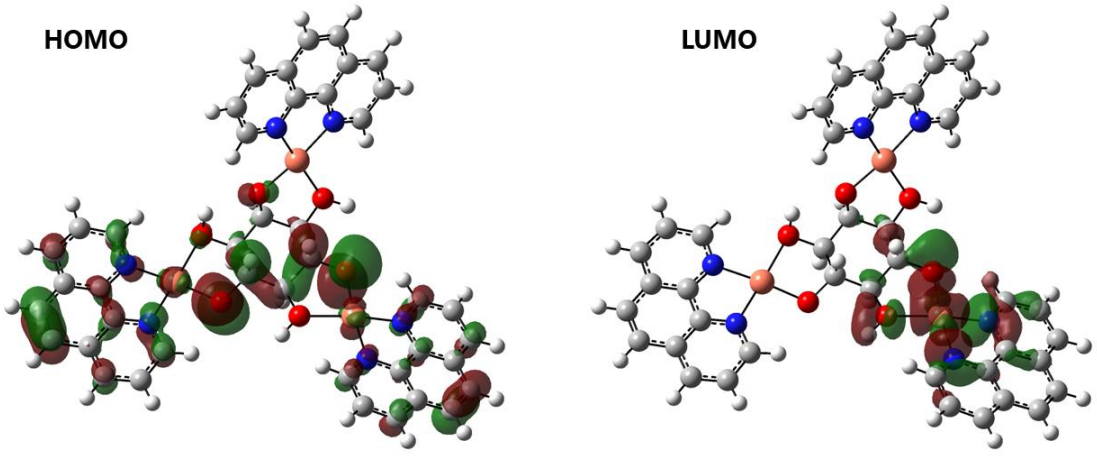

Figure 5.3.7.2 The HOMO and LUMO for the metallogelator complex [$Cu_3(H_3ins)(phen)_3$]$^{3+}$.

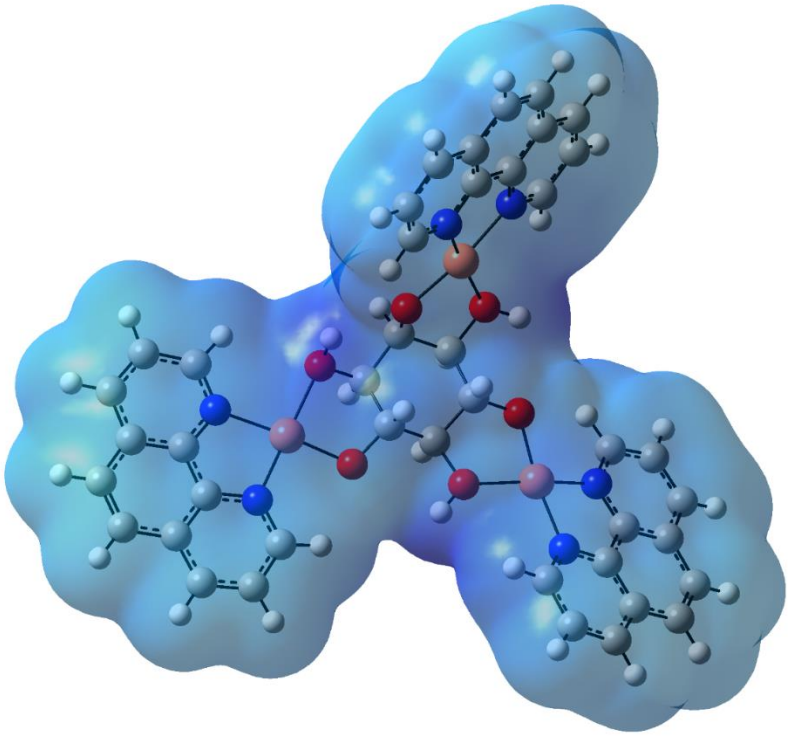

Figure 5.3.7.3 The ESP plots of the metallogelator complex [**$Cu_3(H_3ins)(phen)_3]^{3+}$**.

The ESP plots and the energy gap (ΔE_g) have been represented in the **Figure 5.3.7.3** and **Table 5.3.7.1,** respectively. The energy gap (ΔE_g), E_{HOMO} and E_{LUMO} values are important for the prediction of global reactivity descriptors, which in details explain the internal charge transfer, stability and reactivity of the molecule[23]. Global reactivity descriptors such as **electronegativity (χ), global hardness (η), global electrophilicity (ω)** and **global softness (σ)** are calculated using the formulas based on Koopmans theorem[24] and are tabulated **(Table 5.3.7.1).**

$$Electronegativity\ (\chi) = -{}^{1}/_{2}\ (I + A)$$

$$Global\ Hardness\ (\eta) = {}^{1}/_{2}\ (I - A)$$

$$Chemical\ Potential\ (\mu) = {}^{1}/_{2}\ (E_{HOMO} + E_{LUMO})$$

$$Global\ Softness\ (S) = 1/2\eta$$

$$Electrophilicity\ (\omega) = {}^{\mu^2}/_{2\eta}$$

The energy gap (ΔE_g) value is directly associated with the stability and hardness and inversely related with the reactivity and softness of the molecule. A very small energy

gap value shows that there is an easy charge transfer within the molecule, which may further increase the biological activity of the complex.

Table 5.3.7.1 Global reactivity descriptors of complexes in eV calculated by DFT/B3LYP/LANL2DZ basis set for **$[Cu_3(H_3ins)(phen)_3]^{3+}$ and $[Cu_3(H_3ins)(ins)_3]^{3+}$.**

Molecular Properties	Mathematical Description	Values for $[Cu_3(H_3ins)(phen)_3]^{3+}$	Values for $[Cu_3(H_3ins)(neo)_3]^{3+}$
E_{HOMO}	Energy of HOMO	**-12.865**	**-12.721**
E_{LUMO}	Energy of LUMO	**-9.860**	**-9.937**
Energy gap	$\Delta E_g = E_{LUMO} - E_{HOMO}$	**3.005**	**2.784**
Ionization potential (IP)	$IP = -E_{HOMO}$	**12.865**	**12.721**
Electron Affinity (EA)	$EA = -E_{LUMO}$	**9.860**	**9.937**
Electronegativity (χ)	$\chi = -\frac{1}{2}(E_{HOMO} + E_{LUMO})$	**11.3625**	**11.329**
Chemical Potential (μ)	$\mu = \frac{1}{2}(E_{HOMO} + E_{LUMO})$	**-11.3625**	**-11.329**
Global Hardness (η)	$\eta = -\frac{1}{2}(E_{HOMO} - E_{LUMO})$	**1.5025**	**1.392**
Softness (S)	$S = 1/2\eta$	**0.33277**	**0.348**
Electrophilicity index (ω)	$\omega = \mu^2/2\eta$	**42.963**	**46.101**

As per the computation, the molecule is an asymmetric top, however, has near C_3 symmetry. It can be seen from the values in **Table 5.3.7.2** and **Figure 5.3.7.1** that the torsional angles around copper(II) are between ~175-190 degrees, bond angles are approximately ~ 90 degrees, these features indicate that the coordination geometry around copper is approximately planar. However, as the bond angles are not exaclty 90° the geometry around copper(II) centers is not exactly square planar, it is slightly distorted. These geometrical features should facilitate π-π stacking. Also the near planar coordination geometry makes the inositol oxygens available for H-bonding with solvent and for an interaction with anions.

Table 5.3.7.2 Optimized geometrical parameters involving metal coordination for the metallogelator complex **$[Cu_3(H_3ins)(phen)_3]^{3+}$**.

Cu-N Distances (A^o)		
R(24,76)	N24-Cu76	**2.0296**
R(32,76)	N32-Cu76	**2.0042**
R(58,77)	N58-Cu77	**2.0181**
R(64,77)	N64-Cu77	**2.0056**
R(40,78)	N40-Cu78	**2.005**
R(46,78)	N46-Cu78	**2.025**
Cu-O Distances (A^o)		
R(8,76)	O8-Cu76	**2.0753**
R(12,76)	O12-Cu76	**1.9132**
R(7,77)	O7-Cu77	**1.9189**
R(11,77)	O11-Cu77	**2.0951**
R(9,78)	O9-Cu78	**2.051**
R(10,78)	O10-Cu78	**1.9129**
Bond angles		
A(32,76,24)	N32-Cu76-N24	**83.400**
A(8,76,24)	O8-Cu76-N24	**100.396**
A(8,76,12)	O8-Cu76-O12	**84.499**
A(12,76,32)	O12-Cu76-N32	**93.8929**
A(7,77,64)	O7-Cu77-N64	**83.4855**
A(7,77,11)	O7-Cu77-O11	**85.5708**
A(11,77,58)	O11-Cu77-N58	**96.6722**
A(58,77,64)	N58-Cu77-N64	**83.4855**
A(9,78,10)	O9-Cu78-O10	**83.9574**
A(10,78,40)	O10-Cu78-N40	**96.2866**
A(40,78,46)	N40-Cu78-N46	**83.4227**
A(9,78,46)	O9-Cu78-N46	**97.9314**
Torsional angles		
L(12,76,24,8,-1)	O12-Cu76-N24-O8 (-1)	**184.895**
L(7,77,58,64,-1)	O7-Cu77-N58-N64 (-1)	**178.7562**
L(11,77,64,58,-1)	O11-Cu77-N64-N58 (-1)	**180.1577**
L(9,78,40,46,-1)	O9-Cu78-N40-N46 (-1)	**181.3542**
L(10,78,46,40,-1)	O10-Cu78-N46-N40 (-1)	**179.7094**
L(12,76,24,8,-2)	O12-Cu76-N24-O8 (-1)	**187.4283**
L(7,77,58,64,-2)	O7-Cu77-N58-N64 (-2)	**188.3465**
L(11,77,64,58,-2)	O11-Cu77-N64-N58 (-2)	**186.9997**
L(9,78,40,46,-2)	O9-Cu78-N40-N46 (-2)	**191.2078**
L(10,78,46,40,-2)	O10-Cu78-N46-N40 (-2)	**188.2701**

Similarly, the geometry of **$[Cu_3(H_3ins)(neo)_3]^{3+}$** was optimized using DFT theory with B3LYP and LanL2DZ as basis sets **(Figure 5.3.7.4)**. The HOMO and LUMO frontier orbitals have been represented in the **Figure 5.3.7.5.** The ESP plots for the complex

$[Cu_3(H_3ins)(neo)_3]^{3+}$and the energy gap ($\Delta E_g$) have been represented in the **Figure 5.3.7.6** and **Table 5.3.7.1,** respectively. Global reactivity descriptors such as **electronegativity (χ), global hardness (η), global electrophilicity (ω)** and **global softness (σ)** are calculated using the formulas based on Koopmans theorem[23] and are tabulated **(Table 5.3.7.1).**

As per the computation, the molecule is an asymmetric top, however, has near C_3 symmetry. It can be seen from the values in **Table 5.3.7.3** and **Figure 5.3.7.4** that the torsional angles around copper(II) are between ~175-190 degrees, bond angles are approximately ~ 90 degrees, these features indicate that the coordination geometry around copper is approximately planar.

The global reactivity descriptors of complex cations $[Cu_3(H_3ins)(phen)_3]^{3+}$ and $[Cu_3(H_3ins)(neo)_3]^{3+}$ have comparable values as they have similar geometry. The values of HOMO-LUMO gap and other descriptors for $[Cu_3(H_3ins)(neo)_3]^{3+}$ are slightly lower owing to the presence of $-CH_3$ groups.

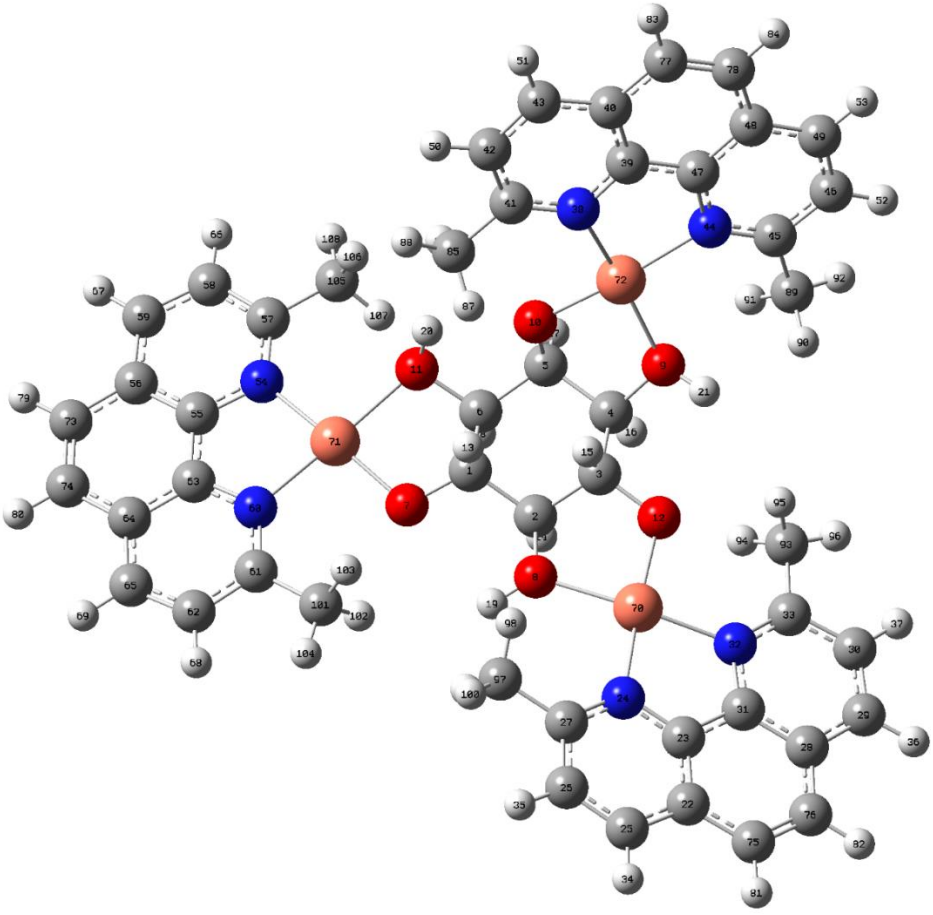

Figure 5.3.7.4 The optimized structure of the complex $[Cu_3(H_3ins)(neo)_3]^{3+}$using B3LYP theory and LanL2DZ as basis sets.

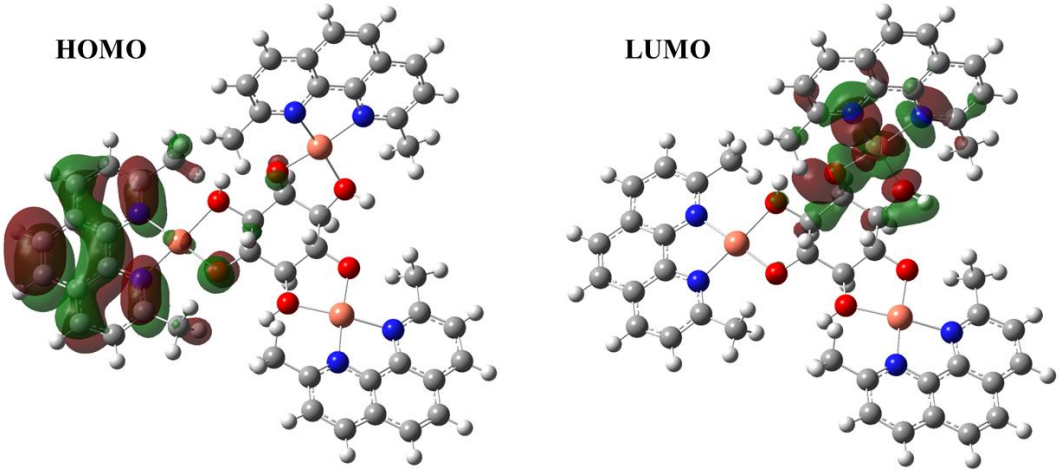

Figure 5.3.7.5 The HOMO and LUMO for the metallogelator complex [**$Cu_3(H_3ins)(neo)_3]^{3+}$**.

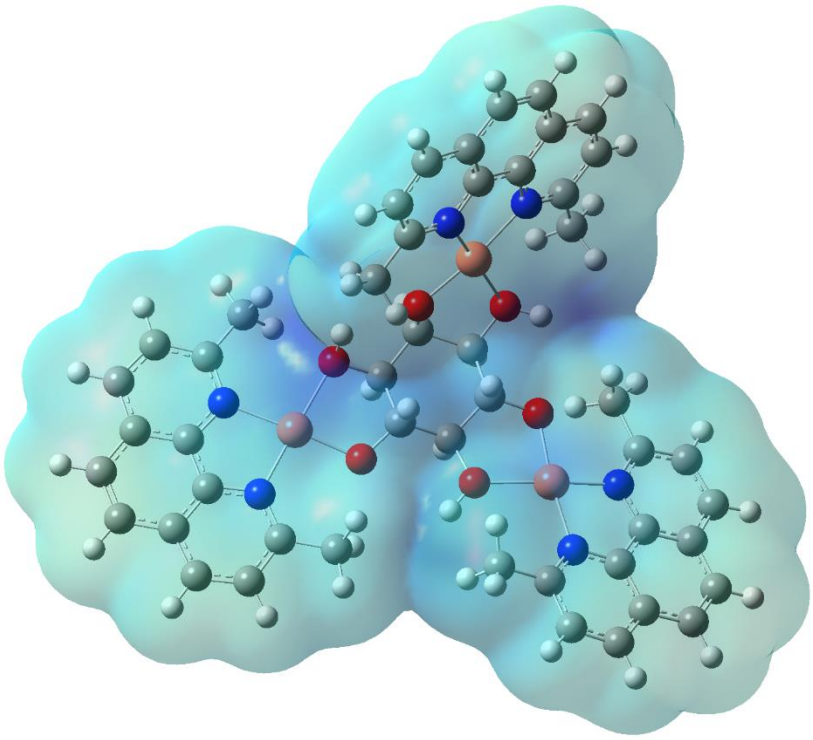

Figure 5.3.7.6 The ESP plots of the metallogelator complex [**$Cu_3(H_3ins)(neo)_3]^{3+}$**.

Table 5.3.7.3 Optimized geometrical parameters involving metal coordination for the metallogelator complex **$[Cu_3(H_3ins)(neo)_3]^{3+}$**.

Cu-N Distances (A^o)		
R(24,70)	N24-Cu70	**2.017**
R(32,70)	N32-Cu70	**2.0016**
R(38,72)	N38-Cu72	**1.9991**
R(44,72)	N44-Cu72	**2.0182**
R(54,71)	N54-Cu71	**2.0075**
R(60,71)	N60-Cu71	**2.0029**
Cu-O Distances (A^o)		
R(8,70)	O8-Cu70	**2.0715**
R(7,71)	O7-Cu71	**1.9127**
R(9,72)	O9-Cu72	**2.0405**
R(10,72)	O10-Cu72	**1.9105**
R(11,71)	O11-Cu71	**2.0875**
R(12,70)	O12-Cu70	**2.0715**
Bond angles		
A(8,70,12)	O8-Cu70-O12	**83.2052**
A(8,70,24)	O8-Cu70-N24	**101.1955**
A(12,70,32)	O12-Cu70-O32	**94.1472**
A(24,70,32)	N24-Cu70-N32	**83.8754**
A(7,71,11)	O7-Cu71-O11	**83.4424**
A(7,71,60)	O7-Cu71-O60	**95.8319**
A(11,71,54)	O11-Cu71-N54	**98.1276**
A(54,71,60)	N54-Cu71-N60	**83.9191**
A(9,72,10)	O9-Cu72-O10	**82.4395**
A(9,72,44)	O9-Cu72-N44	**98.6472**
A(10,72,38)	O10-Cu72-N38	**96.7349**
A(38,72,44)	N38-Cu72-N44	**83.856**
Torsional angles		
L(12,70,24,8,-1)	O12-Cu70-N24-O8 (-1)	**184.4007**
L(7,71,54,60,-1)	O7-Cu71-N54-N60 (-1)	**179.751**
L(11,71,60,54,-1)	O11-Cu71-N60-N54 (-1)	**182.0467**
L(9,72,38,44,-1)	O9-Cu72-N38-N44 (-1)	**182.5032**
L(10,72,44,38,-1)	O10-Cu72-N44-N38 (-1)	**180.5908**
L(12,70,24,8,-2)	O12-Cu70-N24-O8 (-1)	**188.1533**
L(7,71,54,60,-2)	O7-Cu71-N54-N60 (-2)	**189.5826**
L(11,71,60,54,-2)	O11-Cu71-N60-N54 (-2)	**187.854**
L(9,72,38,44,-2)	O9-Cu72-N38-N44 (-2)	**191.3539**
L(10,72,44,38,-2)	O10-Cu72-N44-N38 (-2)	**188.4118**

5.3.8 Microscopic Properties

Scanning Electron Microscopy of metallogels (SEM)

One of the distinct morphological characteristics of the gels is the presence of fibrous assembly spread throughout the metallogelator network in 3 dimensions. Gel is a network of immobile solvent trapped in the framework of the solid compound/complex. The gelator system is held together because of the presence of the fibrous assembly, which is formed owing to the different non-covalent interactions like π-π stacking and intermolecular H-bonding between the metallogelator complex molecules.

The metallogels **231, 232, 251, 252** and **332** considered for study in this chapter were analyzed using SEM analysis. The gels were dried and converted into xerogels before recording the SEM analysis. The SEM images reveal the presence of fibrous assemblies in each of these metallogels (**Figure 5.3.8.1** and **Figure 5.3.8.2**).

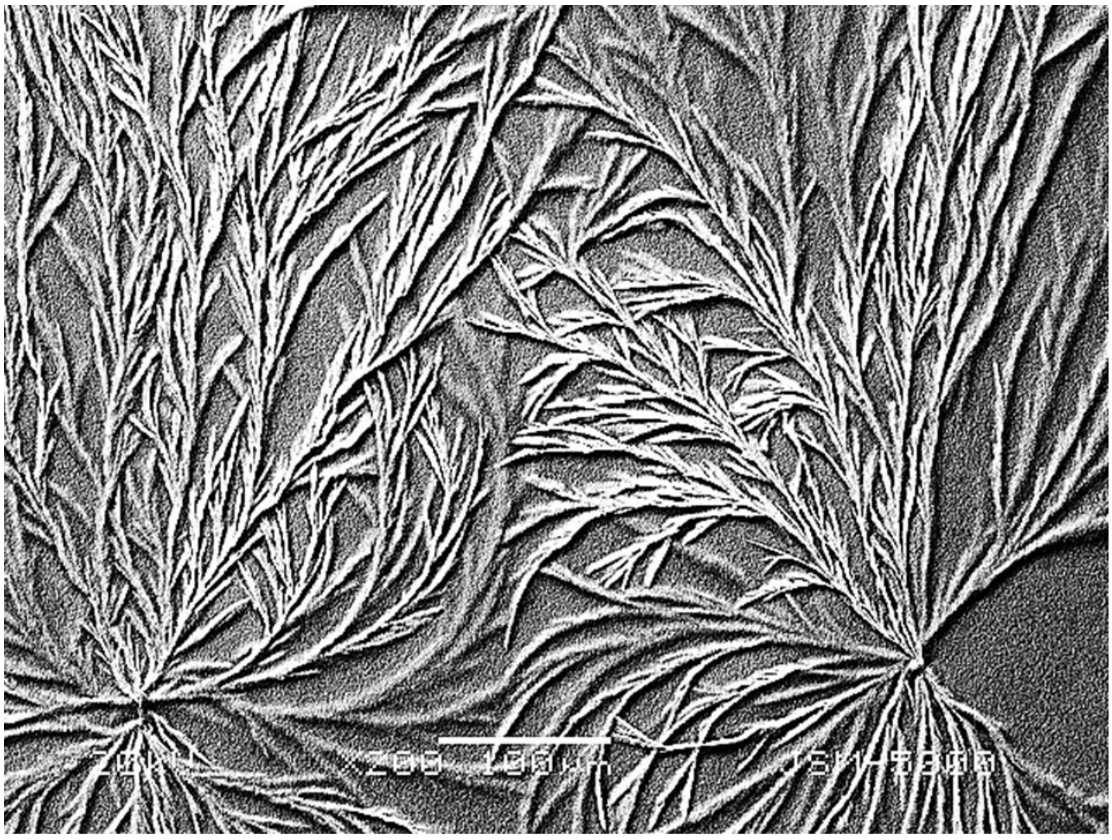

Figure 5.3.8.1 SEM images of xerogels showing the fibrous assemblies in the metallogel **232**.

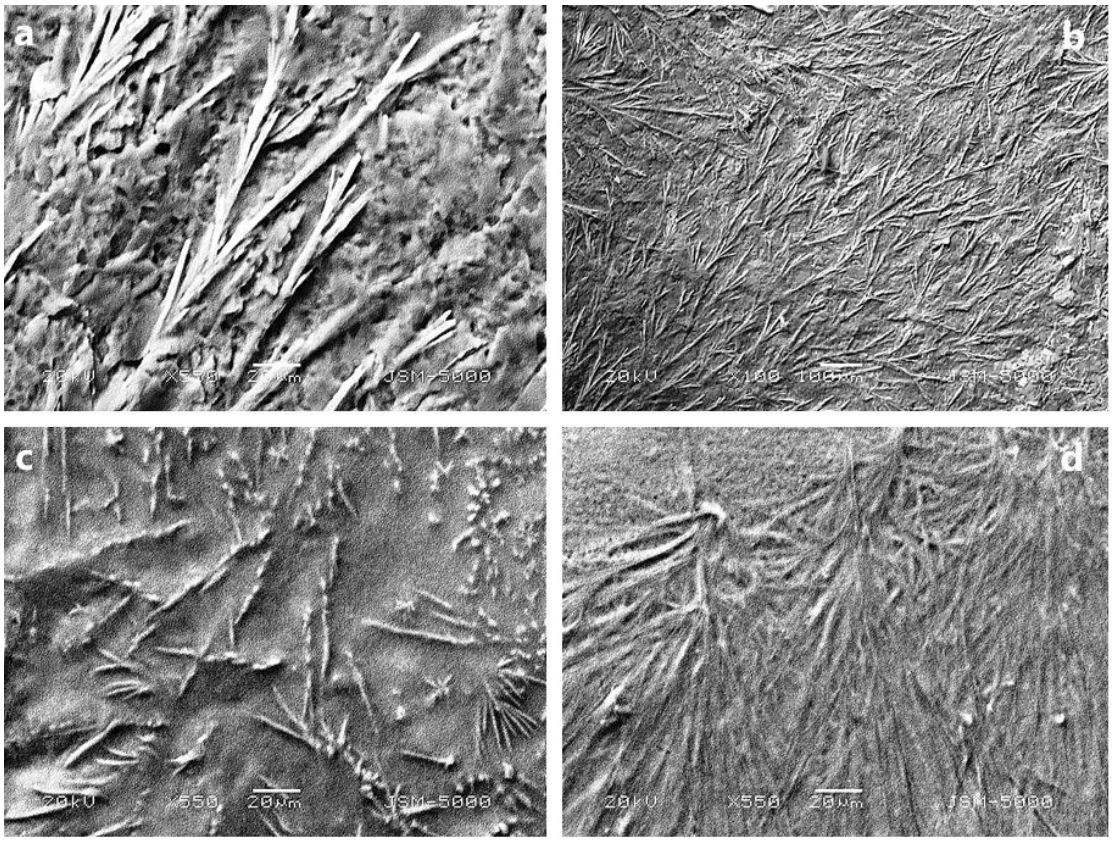

Figure 5.3.8.2 SEM images of xerogels **(a) 231, (b) 251, (c) 252** and **(d) 332** showing the fibrous assembly of the metallogels.

Polarizing Optical Microscopy (POM)

The gel forming complex, being trinuclear has to be dissymmetric having at the most a C_3 symmetry axis. This can induce chirality in the molecule which can further get enhanced by the stacking of molecules and the formation of supramolecular assembly and thus can attribute birefringent property to the gels. In order to examine this possibility and any temperature dependent behaviour, polarizing microscopic studies of the xerogels were carried out. Similar microscopic patterns as reported in chapters 2 and 4 were observed here.

In order to perform the POM of the xerogels, a drop of the gel was placed on a slide and allowed to dry and convert to a xerogel. The solution of the complex was isotropic and as it gradually changes to a gel, it gets organized and displays birefringent anisotropic behavior on conversion to a xerogel. It was observed that the appearance of the birefringent structures/patterns in the metallogels was temperature independent phenomenon. This behavior, however, was seen to be dependent on the solvent immobilized by the supramolecular assembly and the birefringent patterns could only be observed when the solvent, water in this case, was lost by the gels and they got

converted to xerogels. The phenomenon is reversible on removal and exposure to moisture.

Birefrigent properties of metallogels

The birefringent property of the gels arising due to the dissymmetry in the complex ion was explored at different angles of polarizer and analyzer using POM. One of the characteristic properties of birefringent materials is that they respond to the change in the angle between polarizer and the analyzer. The images were captured at different angles of the polarizer and the analyzer **(0, 45, 90, 135).** It was observed from the images recorded at different angles of polarizer that the assembly is highly birefringent, such behavior of the gels as discussed in the present chapter is unique **(Figure 5.3.8.3 to Figure 5.3.8.6)** and similar to that observed in case of xerogels having bipy as capping agent.

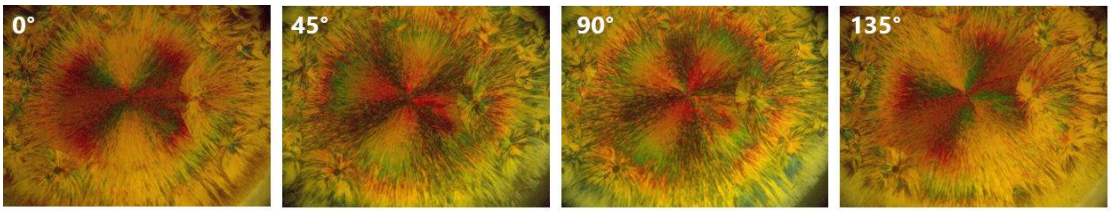

Figure 5.3.8.3 Birefringence and angle dependent POM images of xerogel **231**, **(0, 45, 90, 135)** written after the gel codes on the top right corner in the images represent the angles of polarizer in degrees).

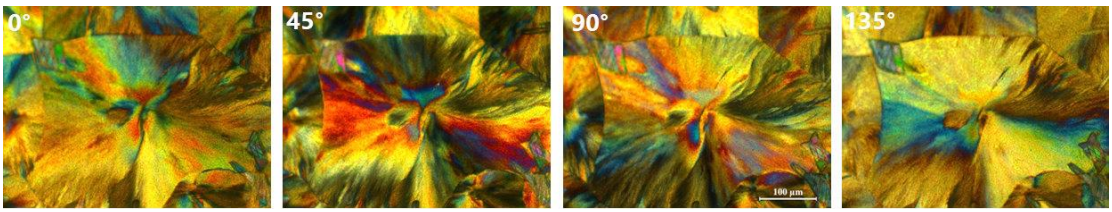

Figure 5.3.8.4 Birefringence and angle dependent POM images of xerogel **232**, **(0, 45, 90, 135)** written after the gel codes on the top right corner in the images represent the angles of polarizer in degrees).

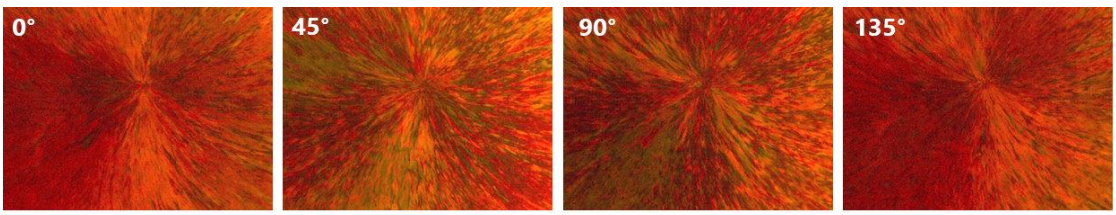

Figure 5.3.8.5 Birefringence and angle dependent POM images of xerogel **251**, **(0, 45, 90, 135)** written after the gel codes on the top right corner in the images represent the angles of polarizer in degrees).

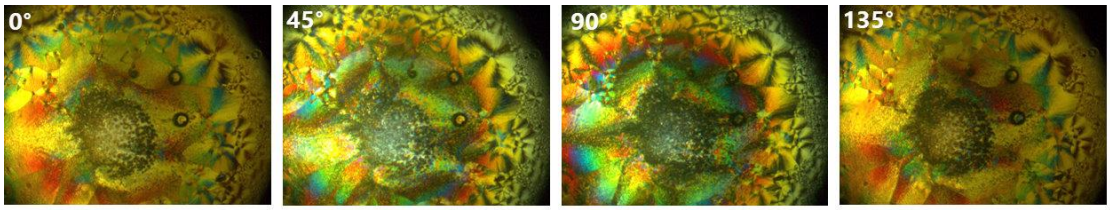

Figure 5.3.8.6 Birefringence and angle dependent POM images of xerogel **252**, **(0, 45, 90, 135)** written after the gel codes on the top right corner in the images represent the angles of polarizer in degrees).

5.3.9 Solvent uptake studies of metallogels

The metallogels reported in the present chapter and the previous chapters are all hydrogels, meaning that they incorporate water in the immobile 3-D network formed by the metallogelator complexes in presence of carbonate or hydroxide bases. The formation of gel takes place due to the non-covalent interactions like H-bonding and π-π stacking. However, apart from these interactions and many other factors like temperature, pH etc., the type and the amount of the solvent plays a major role in deciding the stability as well as other morphological properties of the metallogels. The dimensions of the fibrous assembly resulting in the metallogel formation well as properties like T_{gel} depend on the type and the quantity of the solvent incorporated.

The metallogels reported in Chapter 2 had bipy as the capping agent while those reported in the present chapter have phen as the capping agent. As the capping agent were varied from bipy to 1,10-phenanthroline and their derivatives, the aromatic character and /or hydrophobicity of the exterior part of the gelator molecules increased. Hence, it was thought of interest to explore the uptake of organic solvents by metallogels.

Gel formation in presence of organic solvents

The gel formation was tried in presence of a variety of polar and non-polar organic solvents like methanol, ethanol, DMF, DMSO, diethyl ether, THF and acetonitrile. The experiments were also carried out to check the capacity of preformed gels to incorporate another solvent.

A striking observation was made that gels did not form in presence of any other solvent added initially, before the gel formation but once the metallogels are formed, they can encapsulate various organic solvents. The observations are summarized in **Table 5.3.9.1 to Table 5.3.9.4**.

Table 5.3.9.1 The solvent uptake capacities of Gel-222

Solvent	Ratio (Gel:Solvent)	Result
Methanol	**1:1**	**Gel**
Methanol	**1:2**	**Gel**
Methanol	**1:5**	**Gel**
Methanol	**1:10**	**Gel**
Methanol	**1:20**	**Gel (supergelator)**
Ethanol	**1:1**	**Gel**
Ethanol	**1:2**	**Gel**
Ethanol	**1:3**	**Gel**
Ethanol	**1:5**	**Gel**
DMSO	**1:1**	**Gel**
DMSO	**1:2**	**Gel**
DMF	**1:1**	**Gel**
DMF	**1:2**	**Gel**
THF	**1:1**	**No Gel**
Acetonitrile	**1:1**	**Gel**
Diethyl ether	**1:1**	**No Gel**

The solvent uptake capacities for metallogels **222** and **232** have been shown in the **Table 5.3.9.1** and **Table 5.3.9.2,** respectively. It can be observed that the uptake capacity of both of these gels, especially, for methanol is exceptionally high. The gels can incorporate approximately **20 times** the volume of methanol **(0.75 w/w %)** of their original volume at room temperature **(Figure 5.3.9.1)**. Both the gels **(232, 222)** can be considered as supergelators in terms of their solvent uptake capacity for methanol.

Table 5.3.9.2 The solvent uptake capacities of Gel-232

Solvent	Ratio (Gel:Solvent)	Result
Methanol	1:1	Gel
Methanol	1:2	Gel
Methanol	1:5	Gel
Methanol	1:10	Gel
Methanol	1:20	Gel (supergelator)
Ethanol	1:1	Gel
Ethanol	1:2	Gel
DMSO	1:1	Gel
DMSO	1:2	Gel
DMF	1:1	Gel
THF	1:1	No Gel
Acetonitrile	1:1	No Gel
Diethyl ether	1:1	No Gel

Figure 5.3.9.1 The uptake of methanol by the metallogel-232 and the images of the gel under SEM.

The metallogels **232** and **222** are formed by the complex $[Cu_3(H_3ins)(phen)_3](CH_3COO)_3$ in presence of K_2CO_3 and KOH, respectively, the only difference being the alkali used in the formation of supramolecular assembly. As the gel forming complex for both the metallogels is the same, the solvent uptake capacity of both the gels in terms of nature and quantity of solvents that could be entrapped is almost the same, with an exception of **acetonitrile** and **DMSO**. Acetonitrile could be entrapped in the metallogel **222** but not in **232**. Metallogel **222** was able to entrap DMSO upto **1:2** ratio **(Table 5.3.9.1),** while gel **232** can uptake only equal volume (1:1 ratio) of DMSO **(Table 5.3.9.2)**.

The experiments to incorporate various organic solvents in the gels **122** and **132** were also successful **(Table 5.3.9.3** and **Table 5.3.9.4)**, however, the amount of solvents that can be incorporated in these gels without converting them in the solutions is much less as compared to **222** and **232**. Both metallogels, **122** and **132**, have 2,2'-bipyridine as capping ligand which has less hydrophobic character as compared to 1,10-phenanthroline which must be responsible for lower solvent uptake capacity of these gels as compared to **222** and **232**. Gel **122** could entrap methanol, ethanol, DMF and DMSO while gel **132** could entrap only methanol, ethanol and DMSO.

Table 5.3.9.3 The solvent uptake capacities of Gel-122

Solvent	Ratio (Gel:Solvent)	Result
Methanol	**1:1**	**Gel**
Methanol	**1:2**	**Gel**
Ethanol	**1.5:1**	**Gel**
DMSO	**1.5:1**	**Gel**
DMSO	**1:1**	**Gel**
DMF	**1.5:1**	**Gel**
DMF	**3:1**	**Gel**
THF	**1:1**	**No Gel**
Acetonitrile	**1:1**	**No Gel**
Diethyl ether	**1:2**	**No Gel**
Diethyl ether	**1:1**	**No Gel**

Table 5.3.9.4 The solvent uptake capacities of Gel-132

Solvent	Ratio (Gel:Solvent)	Result
Methanol	**1:1**	**Gel**
Ethanol	**1.5:1**	**Gel**
DMSO	**3:1**	**Gel**
DMF	**3:1**	**No Gel**
THF	**3:1**	**No Gel**
Acetonitrile	**3:1**	**No Gel**
Diethyl ether	**1:1**	**No Gel**

It was also observed that the gel formation does not take place if any of these solvents were added to the gel forming mixture prior to the formation of metallogels. The gel formation was neither successful in an organic solvent nor in a mixture of water and organic solvent. Only the preformed metallogels were able to uptake different solvents. This is a very striking example which shows that these gels once formed, themselves can act as organo-gelators.

Effect of Solvent on the T_{gel} values

Table 5.3.9.5 T_{gel} values of the gel 232 with change in solvents.

Solvent	Volume of gel(µL)	Volume of solvent(µL)	T_{gel} (°C)
Methanol	250	500	**67** ± 0.5
Ethanol	250	500	**65** ± 0.5
DMSO	250	500	**57** ± 0.5
Water	250	-	**37** ± 0.5

The dependence of T_{gel} on the type of solvents and the quantity of the solvents entrapped was studied. T_{gel} values depend on the strength of interactions present between the gelator molecules as well as the gelator molecules and the solvent. As the solvent changes, the strength of interaction with solvents, specially the solvent dependent interations like π-π stacking and hydrophobic interaction, changes. This results in the variation of the T_{gel}.

The $\mathbf{T_{gel}}$ measurements in presence of different solvents were carried out for the metallogel **232** which is shown in the **Table 5.3.9.5**. The strongest gels are formed in presence of methanol and ethanol, which is also indicated by the amount of these solvents the gel can uptake. It was also observed that as the methanol uptake of the gel increases the gels become more rigid and **no sol-gel transition** was observed till 100º C, which is well beyond the boiling point of methanol.

5.4 Conclusions

- Attempts were made to form gels by using different capping ligands like 1,10-phenanthroline, neocuproine (2,9-dimethyl-1,10-phenanthroline), 3,4,7,8-tetramethyl 1,10-phenanthroline, biquinoline and 6,6'-dimethyl-2,2'-bipyridine in place of 2,2'-bipyridine in the gel forming trinuclear complex.
- The gel formation could be achieved in all except 5-Nitro-1,10-phenanthroline and biquinoline. This can be mainly attributed to the presence of nitro group which is more polar and can provide additional H-binding sites thus probably hindering with the π-π stacking interaction between the phenanthroline moieties.
- The metallogels having phenanthroline as capping ligands and synthesized using carbonate bases are capable to further uptake a variety of organic solvents like methanol, ethanol, DMSO and DMF.
- The metallogels synthesized using caustic alkali were even more versatile than the carbonate gels and they could even uptake CH_3CN and THF in addition to other solvents mentioned above.
- Further, the T_{gel} properties were also dependent on the nature and the amount of solvent incorporated.
- The phenanthroline gels have a tremendous solvent uptake capacity, especially methanol. They can absorb 20 times the volume of methanol (0.75 w/w %) of their original volume at room temperature thus behaving as supergelators.

References

1. Abdallah, B. D. J. & Weiss, R. G. Organogels and Low Molecular Mass Organic Gelators. *Adv. Mater.* **12**, 1237–1247 (2000).

2. Terech, P. & Weiss, R. G. Low Molecular Mass Gelators of Organic Liquids and the Properties of Their Gels. *Chem. Rev.* **2665**, 3133−3159 (1997).

3. *Molecular Gels: Materials With Self- Assembled Fibrillar Networks, (Eds. R. G. Weiss and P. Terech)*. (Springer, Dordrecht, 2006).

4. Dastidar, P. Supramolecular gelling agents : can they be designed ? *Chem. Soc. Rev.* **37**, 2699–2715 (2008).

5. Esch, J. H. Van & Feringa, B. L. New Functional Materials Based on Self-Assembling Organogels : From Serendipity towards Design. *Angew. Chem. Int. Ed.* **39**, 2263–2266 (2000).

6. Xing, B., Choi, M. F. & Xu, B. A stable metal coordination polymer gel based on a calix[4]arene and its “uptake” of non-ionic organic molecules from the aqueous phase. *Chem. Commun.* 362–363 (2002).

7. Estroff, L. A. & Hamilton, A. D. Water Gelation by Small Organic Molecules Lara. *Chem. Rev.* **104**, 1201–1218 (2004).

8. Babu, S. S., Praveen, V. K. & Ajayaghosh, A. Functional π-gelators and their applications. *Chem. Rev.* **114**, 1973–2129 (2014).

9. Fenniri, H., Mathivanan, P., Vidale, K. L., Sherman, D. M., Hallenga, K., Wood, K. V. & Stowell, J. G. Helical rosette nanotubes: Design, self-assembly, and characterization. *J. Am. Chem. Soc.* **123**, 3854–3855 (2001).

10. Israelachvili, J. N. *Intermolecular and Surface Forces*. (Academic Press, New York, 3rd edn, 1991).

11. Ajayaghosh, A. & George, S. J. First phenylenevinylene based organogels: Self-assembled nanostructures via cooperative hydrogen bonding and π-stacking. *J. Am. Chem. Soc.* **123**, 5148–5149 (2001).

12. Raeburn, J., Mendoza-Cuenca, C., Cattoz, B. N., Little, M. A., Terry, A. E., Zamith Cardoso, A., Griffiths, P. C. & Adams, D. J. The effect of solvent choice on the gelation and final hydrogel properties of Fmoc-diphenylalanine. *Soft Matter* **11**, 927–935 (2015).

13. Vosko, S. H., Wilk, L. & Nusair, M. Accurate spin-dependent electron liquid correlation energies for local spin density calculations: a critical analysis. *Can. J. Phys.* **58**, 1200–1211 (1980).

14. Stephens, P. J., Devlin, F. J., Chabalowski, C. F. & Frisch, M. J. Ab Initio calculation of vibrational absorption and circular dichroism spectra using density functional force fields. *J. Phys. Chem.* **98**, 11623–11627 (1994).

15. Becke, A. D. Density-functional thermochemistry. III. The role of exact exchange. *J. Chem. Phys.* **98**, 5648–5652 (1993).

16. Lee, C., Yang, W. & Parr, R. G. Development of the Colle-Salvetti correlation-

energy formula into a functional of the electron density. *Physcial Rev. B* **37**, 785–789 (1988).

17. McLean, A. D. & Chandler, G. S. Contracted Gaussian basis sets for molecular calculations. I. Second row atoms, Z=11-18. *J. Chem. Phys.* **72**, 5639–5648 (1980).

18. Krishnan, R., Binkley, J. S., Seeger, R. & Pople, J. A. Self-consistent molecular orbital methods. XX. A basis set for correlated wave functions. *J. Chem. Phys.* **72**, 650–654 (1980).

19. Frisch, M. J., Trucks, G. W., Schlegel, H. B., Scuseria, G. E., Robb, M. A., Cheeseman, J. R., Scalmani, G., Barone, V., Petersson, G. A., Nakatsuji, H., Li, X., Caricato, M., Marenich, A. V, Bloino, J., Janesko, B. G., Gomperts, R., Mennucci, B., Hratchian, H. P., *et al.* Gaussian 16, Revision A.03. *Gaussian, Inc., Wallingford CT* (2016).

20. Dennington, R., Keith, T. A. & Millam, J. M. GaussView 6. (2016).

21. Gouda, A. A. & Amin, A. S. Copper(II)-neocuproine reagent for spectrophotometric determination of captopril in pure form and pharmaceutical formulations. *Arab. J. Chem.* **3**, 159–165 (2010).

22. Fukui, K. Role of Frontier Orbitals in Chemical Reactions. *Science (80-.).* **218**, 747–754 (1982).

23. Jawaria, R., Hussain, M., Khalid, M., Khan, M. U., Tahir, M. N., Naseer, M. M., Braga, A. A. C. & Shafiq, Z. Synthesis, crystal structure analysis, spectral characterization and nonlinear optical exploration of potent thiosemicarbazones based compounds: A DFT refine experimental study. *Inorganica Chim. Acta* **486**, 162–171 (2019).

24. Koopmans, T. Über die Zuordnung von Wellenfunktionen und Eigenwerten zu den Einzelnen Elektronen Eines Atoms. *Physica* **1**, 104–113 (1934).

•

Chapter 5

Effect of capping agents on gel formation and uptake of organic solvents by metallogels derived from 1,10- phenanthroline containing tricopper(II) complex